

Supporting Information

Regio-specific Enzymatic Glucosylation of Triterpenoids from *Antrodia camphorata* and their Biological Activities

Hui-Fei Su,^{‡a} Bin Li,^{‡a,b} Yang Yi,^a Meng Zhang,^a Rong Yu,^a Yang-Oujie Bao,^a Kuan
Chen^a and Min Ye^{*a,c}

^a State Key Laboratory of Natural and Biomimetic Drugs & Key Laboratory of
Molecular Cardiovascular Sciences of Ministry of Education, School of Pharmaceutical
Sciences, Peking University, 38 Xueyuan Road, Beijing 100191, China

^b Key Laboratory of Bioactive Substances and Resources Utilization of Chinese Herbal
Medicine, Ministry of Education, Institute of Medicinal Plant Development, Chinese
Academy of Medical Sciences, Peking Union Medical College, Beijing 100193, China

^c Yunnan Baiyao International Medical Research Center, Peking University, 38
Xueyuan Road, Beijing 100191, China

* Corresponding author. Fax: (+86)-10-8280-2024.

E-mail address: yemin@bjmu.edu.cn (M. Ye)

[‡] These authors contributed equally to this work.

Contents

Experimental

1. General
2. YjiC1 expression and purification
3. Enzyme catalytic activity assay at the analytical scale
4. Preparative-scale enzymatic reactions of **1-7** and **9-10**.
5. Structural characterization
6. Inhibition activities against COX-2
7. Lipopolysaccharide (LPS)-induced acute lung injury (ALI) mice model
8. Pathological analysis
9. Immunohistochemistry (IHC)

Tables

Table S1. ^1H NMR Spectroscopic Data (in pyridine- d_5) for Compounds **1a-7a**, **9a-9c**, and **10a** (δ in ppm, J in Hz).

Table S2. ^{13}C NMR Spectroscopic Data (in pyridine- d_5) for Compounds **1a-7a**, **9a-9c**, and **10a** (δ in ppm).

Figures

Figure S1. SDS-PAGE analysis of purified YjiC1 protein.

Figure S2. Structures of **12-17** that could not be catalyzed by YjiC1.

Figure S3. HPLC chromatograms of catalytic products by YjiC1 and the substrates.

UV wavelength, 254 nm.

Figure S4. Effects of compounds **4a** and **4** on the mRNA expressions of IL-1 β in the mice lung tissues.

Figure S5. ^1H NMR spectrum of **1a** in pyridine- d_5 (400 MHz).

Figure S6. ^{13}C NMR spectrum of **1a** in pyridine- d_5 (100 MHz).

Figure S7. DEPT 135 spectrum of **1a** in pyridine- d_5 (100 MHz).

Figure S8. HSQC spectrum of **1a** in pyridine- d_5 (400 MHz).

Figure S9. HMBC spectrum of **1a** in pyridine- d_5 (400 MHz).

Figure S10. HR-ESI-MS spectrum of **1a**.

Figure S11. ^1H NMR spectrum of **2a** in pyridine- d_5 (400 MHz).

Figure S12. ^{13}C NMR spectrum of **2a** in pyridine- d_5 (100 MHz).

Figure S13. DEPT 135 spectrum of **2a** in pyridine- d_5 (100 MHz).

Figure S14. HSQC spectrum of **2a** in pyridine- d_5 (400 MHz).

Figure S15. HMBC spectrum of **2a** in pyridine- d_5 (400 MHz).

Figure S16. HR-ESI-MS spectrum of **2a**.

Figure S17. ^1H NMR spectrum of **3a** in pyridine- d_5 (400 MHz).

Figure S18. ^{13}C NMR spectrum of **3a** in pyridine- d_5 (100 MHz).

Figure S19. DEPT 135 spectrum of **3a** in pyridine- d_5 (100 MHz).

Figure S20. HSQC spectrum of **3a** in pyridine- d_5 (400 MHz).

Figure S21. HMBC spectrum of **3a** in pyridine- d_5 (400 MHz).

Figure S22. HR-ESI-MS spectrum of **3a**.

Figure S23. ^1H NMR spectrum of **4a** in pyridine- d_5 (400 MHz).

Figure S24. ^{13}C NMR spectrum of **4a** in pyridine- d_5 (100 MHz).

Figure S25. DEPT 135 spectrum of **4a** in pyridine- d_5 (400 MHz).

Figure S26. HSQC spectrum of **4a** in pyridine- d_5 (400 MHz).

Figure S27. HMBC spectrum of **4a** in pyridine- d_5 (400 MHz).

Figure S28. HR-ESI-MS spectrum of **4a**.

Figure S29. ^1H NMR spectrum of **5a** in pyridine- d_5 (400 MHz).

Figure S30. ^{13}C NMR spectrum of **5a** in pyridine- d_5 (100 MHz).

Figure S31. DEPT 135 spectrum of **5a** in pyridine- d_5 (100 MHz).

Figure S32. HSQC spectrum of **5a** in pyridine- d_5 (400 MHz).

Figure S33. HMBC spectrum of **5a** in pyridine- d_5 (400 MHz).

Figure S34. HR-ESI-MS spectrum of **5a**.

Figure S35. ^1H NMR spectrum of **6a** in pyridine- d_5 (400 MHz).

Figure S36. ^{13}C NMR spectrum of **6a** in pyridine- d_5 (100 MHz).

Figure S37. DEPT 135 spectrum of **6a** in pyridine- d_5 (100 MHz).

Figure S38. HSQC spectrum of **6a** in pyridine- d_5 (400 MHz).

Figure S39. HMBC spectrum of **6a** in pyridine- d_5 (400 MHz).

Figure S40. HR-ESI-MS spectrum of **6a**.

Figure S41. ^1H NMR spectrum of **7a** in pyridine- d_5 (400 MHz).

Figure S42. ^{13}C NMR spectrum of **7a** in pyridine- d_5 (100 MHz).

Figure S43. DEPT 135 spectrum of **7a** in pyridine- d_5 (100 MHz).

Figure S44. HSQC spectrum of **7a** in pyridine- d_5 (400 MHz).

Figure S45. HMBC spectrum of **7a** in pyridine-*d*₅ (400 MHz).

Figure S46. HR-ESI-MS spectrum of **7a**.

Figure S47. ¹H NMR spectrum of **9a** in pyridine-*d*₅ (600 MHz).

Figure S48. ¹³C NMR spectrum of **9a** in pyridine-*d*₅ (150 MHz).

Figure S49. DEPT 135 spectrum of **9a** in pyridine-*d*₅ (150 MHz).

Figure S50. HSQC spectrum of **9a** in pyridine-*d*₅ (600 MHz).

Figure S51. HMBC spectrum of **9a** in pyridine-*d*₅ (600 MHz).

Figure S52. HR-ESI-MS spectrum of **9a**.

Figure S53. ¹H NMR spectrum of **9b** in pyridine-*d*₅ (400 MHz).

Figure S54. ¹³C NMR spectrum of **9b** in pyridine-*d*₅ (100 MHz).

Figure S55. DEPT 135 spectrum of **9b** in pyridine-*d*₅ (100 MHz).

Figure S56. HSQC spectrum of **9b** in pyridine-*d*₅ (400 MHz).

Figure S57. HMBC spectrum of **9b** in pyridine-*d*₅ (400 MHz).

Figure S58. HR-ESI-MS spectrum of **9b**.

Figure S59. ¹H NMR spectrum of **9c** in pyridine-*d*₅ (400 MHz).

Figure S60. ¹³C NMR spectrum of **9c** in pyridine-*d*₅ (100 MHz).

Figure S61. DEPT 135 spectrum of **9c** in pyridine-*d*₅ (100 MHz).

Figure S62. HSQC spectrum of **9c** in pyridine-*d*₅ (400 MHz).

Figure S63. HMBC spectrum of **9c** in pyridine-*d*₅ (400 MHz).

Figure S64. HR-ESI-MS spectrum of **9c**.

Figure S65. ¹H NMR spectrum of **10a** in pyridine-*d*₅ (600 MHz).

Figure S66. ¹³C NMR spectrum of **10a** in pyridine-*d*₅ (150 MHz).

Figure S67. DEPT 135 spectrum of **10a** in pyridine-*d*₅ (150 MHz).

Figure S68. HSQC spectrum of **10a** in pyridine-*d*₅ (600 MHz).

Figure S69. HMBC spectrum of **10a** in pyridine-*d*₅ (600 MHz).

Figure S70. HR-ESI-MS spectrum of **10a**.

1. General

Compounds **1–17** were isolated from *Antrodia camphorata* by our laboratory, including (25*S*)-antcin K (**1**), (25*R*)-antcin K (**2**), (25*S*)-antcin C (**3**), (25*R*)-antcin C (**4**), antcamphin E (**5**), (25*S*)-camphoratin A (**6**), (25*R*)-camphoratin A (**7**), (25*S*)-camphoratin G (**8**), dehydrosulphurenic acid (**9**), dehydroeburicoic acid (**10**), 15 α -acetyl-dehydrosulphurenic acid (**11**), (25*S*)-antcin G (**12**), (25*S*)-methyl antcinate B (**13**), (25*S*)-antcin H (**14**), antcamphin I (**15**), (25*R*)-antcin D (**16**), and (25*R*)-antcin B (**17**).^[1] UDP-Glc was purchased from Sigma-Aldrich (Shanghai, China). ¹H and ¹³C NMR spectra were obtained on a Bruker AVANCE III-400 instrument (400 MHz for ¹H NMR and 100 MHz for ¹³C NMR) or a Bruker AVANCE III-600 instrument (600 MHz for ¹H NMR and 150 MHz for ¹³C NMR) in pyridine-*d*₅ with TMS as reference. HR-ESI-MS spectra were recorded on a Waters Xevo G2 QTOF spectrometer or a Thermo Scientific Q-Exactive ESI-MS instrument. Semi-preparative HPLC was performed on an Agilent 1200 instrument equipped with a YMC Pack ODS-A column (10 × 250 mm, 5 μ m, YMC Co. Ltd., Japan). COX-2 inhibitor screening kit was purchased from Beyotime Biotechnology Ltd (catalog number S0169).

2. YjiC1 expression and purification

Glycosyltransferase YjiC1 (GenBank Accession Number JX982974) was recombinantly expressed in *E. coli*, and was purified using His-tag affinity chromatography as we had previously reported.^[2] The purity of protein was confirmed by SDS-PAGE analysis (Figure S1).

3. Enzyme catalytic activity assay at the analytical scale

The enzyme catalytic reaction was carried out in 100 μ L reaction buffer (50 mM Tris-HCl, pH 8.0) containing 0.1 mM substrate (dissolved in DMSO), 1 mM UDP-Glc, and 50 μ g of YjiC1 enzyme. After 8 h incubation at 37 $^{\circ}$ C, the reaction was terminated by adding 200 μ L MeOH. The mixture was then centrifuged at 12,000 g for 15 min to remove protein. The supernatant was filtered through a 0.22- μ m nylon membrane, and was analyzed by HPLC. A reaction mixture without UDP-Glc was used as the negative control. The conversion rates (%) were calculated by the HPLC peak area ratios of the products versus the substrates.

4. Preparative-scale enzymatic reactions of 1-7 and 9-10.

(25S)-antcin K (1, 9.9 mg) was dissolved in a final volume of 60 mL buffer solution containing 50 mM Tris-HCl (pH 8.0), 0.04 mM UDP-Glc, and 1.2 mg purified enzyme. The reaction was incubated at 37 $^{\circ}$ C for 8 h, the mixture was then extracted with EtOAc (3 \times 240 mL), and the organic solvent was removed under reduced pressure. The residue was dissolved in 1.0 mL of MeOH and subjected to semi-preparative HPLC to obtain (25S)-antcin K 7-*O*- β -D-glucoside (**1a**, 10.8 mg, 82%).

(25R)-antcin K (2, 9.5 mg) was dissolved in a final volume of 60 mL buffer solution containing 50 mM Tris-HCl (pH 8.0), 0.04 mM UDP-Glc, and 1.2 mg purified enzyme. The reaction was incubated at 37 $^{\circ}$ C for 8 h, the mixture was then extracted with EtOAc (3 \times 240 mL), and the organic solvent was removed under reduced pressure.

The residue was dissolved in 1.0 mL of MeOH and subjected to semi-preparative HPLC to obtain (25*R*)-antcin K 7-*O*- β -D-glucoside (**2a**, 10.1 mg, 80%).

(25*S*)-antcin C (**3**, 9.6 mg) was dissolved in a final volume of 60 mL buffer solution containing 50 mM Tris-HCl (pH 8.0), 0.04 mM UDP-Glc, and 1.2 mg purified enzyme. The reaction was incubated at 37°C for 8 h, the mixture was then extracted with EtOAc (3 \times 420 mL), and the organic solvent was removed under reduced pressure. The residue was dissolved in 1.0 mL of MeOH and subjected to semi-preparative HPLC to obtain (25*S*)-antcin C 7-*O*- β -D-glucoside (**3a**, 10.5 mg, 82%).

(25*R*)-antcin C (**4**, 50 mg) was dissolved in a final volume of 250 mL buffer solution containing 50 mM Tris-HCl (pH 8.0), 0.04 mM UDP-Glc, and 5 mg purified enzyme. The reaction was incubated at 37°C for 8 h, the mixture was then extracted with EtOAc (3 \times 420 mL), and the organic solvent was removed under reduced pressure. The residue was dissolved in 1.0 mL of MeOH and subjected to semi-preparative HPLC to obtain (25*S*)-antcin C 7-*O*- β -D-glucoside (**4a**, 50.2 mg, 75%).

Antcamphin E (**5**, 9.8 mg) was dissolved in a final volume of 60 mL buffer solution containing 50 mM Tris-HCl (pH 8.0), 0.04 mM UDP-Glc, and 1.2 mg purified enzyme. The reaction was incubated at 37°C for 8 h, the mixture was then extracted with EtOAc (3 \times 400 mL), and the organic solvent was removed under reduced pressure. The residue was dissolved in 1.0 mL of MeOH and subjected to semi-preparative HPLC to obtain antcamphin E 7-*O*- β -D-glucoside (**5a**, 11.0 mg, 84%).

(25*S*)-camphoratin A (**6**, 10.4 mg) was dissolved in a final volume of 60 mL buffer solution containing 50 mM Tris-HCl (pH 8.0), 0.04 mM UDP-Glc, and 1.2 mg

purified enzyme. The reaction was incubated at 37°C for 8 h, the mixture was then extracted with EtOAc (3 × 420 mL), and the organic solvent was removed under reduced pressure. The residue was dissolved in 1.0 mL of MeOH and subjected to semi-preparative HPLC to obtain (25*S*)-camphoratin A 7-*O*-β-D-glucoside (**6a**, 10.9 mg, 79%).

(25*R*)-camphoratin A (**7**, 10.0 mg) was dissolved in a final volume of 60 mL buffer solution containing 50 mM Tris-HCl (pH 8.0), 0.04 mM UDP-Glc, and 1.2 mg purified enzyme. The reaction was incubated at 37°C for 8 h, the mixture was then extracted with EtOAc (3 × 420 mL), and the organic solvent was removed under reduced pressure. The residue was dissolved in 1.0 mL of MeOH and subjected to semi-preparative HPLC to obtain (25*R*)-camphoratin A 7-*O*-β-D-glucoside (**7a**, 10.4 mg, 78%).

Dehydrosulphurenic acid (**9**, 20.5 mg, 0.04 mM) was dissolved in a final volume of 190 mL buffer solution containing 50 mM Tris-HCl (pH 8.0), 0.08 mM UDP-Glc, 3.5 mg of purified enzyme. The reaction was incubated at 37 °C for 8 h, the mixture was extracted with EtOAc (3 × 380 mL), then the organic solvent was removed by reduced pressure. The residue was dissolved in 1.0 mL of MeOH and subjected to semi-preparative HPLC to dehydrosulphurenic acid 3-*O*-β-D-glucoside (**9a**, 1.4 mg), dehydrosulphurenic acid 15-*O*-β-D-glucoside (**9b**, 7.6 mg), dehydrosulphurenic acid 3,15-di-*O*-β-D-glucoside (**9c**, 11.0 mg),.

Dehydroeburicoic acid (**10**, 57.5 mg, 0.1 mM) was dissolved in a final volume of 250 mL buffer solution containing 50 mM Tris-HCl (pH 8.0), 0.2 mM UDP-Glc, 4.5

mg of purified enzyme. The reaction was incubated at 37 °C for 8 h, the mixture was extracted with EtOAc (3 × 500 mL), then the organic solvent was removed by reduced pressure. The residue was dissolved in 1.0 mL of MeOH and subjected to semi-preparative HPLC to dehydroeburicoic acid 3-*O*-β-*D*-glucoside (**10a**, 34.8 mg, 45%).

5. Structural characterization

(25*S*)-antcin K 7-*O*-β-*D*-glucoside (1a). white amorphous powder; HR-ESI-MS: *m/z* 649.3594 ([*M*-H]⁻, calcd. for C₃₅H₅₃O₁₁, 649.3588); ¹H NMR (400 MHz, pyridine-*d*₅) and ¹³C NMR (100 MHz, pyridine-*d*₅) data, see Tables S1–S2.

(25*R*)-antcin K 7-*O*-β-*D*-glucoside (2a). white amorphous powder; HR-ESI-MS: *m/z* 649.3582 ([*M*-H]⁻, calcd. for C₃₅H₅₃O₁₁, 649.3588); ¹H NMR (400 MHz, pyridine-*d*₅) and ¹³C NMR (100 MHz, pyridine-*d*₅) data, see Tables S1–S2.

(25*S*)-antcin C 7-*O*-β-*D*-glucoside (3a). white amorphous powder; HR-ESI-MS: *m/z* 631.3483 ([*M*-H]⁻, calcd. for C₃₅H₅₁O₁₀, 631.3482); ¹H NMR (400 MHz, pyridine-*d*₅) and ¹³C NMR (100 MHz, pyridine-*d*₅) data, see Tables S1–S2.

(25*R*)-antcin C 7-*O*-β-*D*-glucoside (4a). white amorphous powder; HR-ESI-MS: *m/z* 631.3482 ([*M*-H]⁻, calcd. for C₃₅H₅₁O₁₀, 631.3482); ¹H NMR (400 MHz, pyridine-*d*₅) and ¹³C NMR (100 MHz, pyridine-*d*₅) data, see Tables S1–S2.

Antcamphin E 7-*O*-β-*D*-glucoside (5a). white amorphous powder; HR-ESI-MS: *m/z* 647.3433 ([*M*-H]⁻, calcd. for C₃₅H₅₂O₁₁, 647.3431); ¹H NMR (400 MHz, pyridine-*d*₅) and ¹³C NMR (100 MHz, pyridine-*d*₅) data, see Tables S1–S2.

(25*S*)-camphoratin A 7-*O*-β-*D*-glucoside (6a). white amorphous powder; HR-

ESI-MS: m/z 649.3589 ($[M-H]^-$, calcd. for $C_{35}H_{53}O_{11}$, 649.3588); 1H NMR (400 MHz, pyridine- d_5) and ^{13}C NMR (100 MHz, pyridine- d_5) data, see Tables S1–S2.

(25R)-camphoratin A 7-O- β -D-glucoside (7a): white amorphous powder; HR-ESI-MS: m/z 649.3579 ($[M-H]^-$, calcd. for $C_{35}H_{53}O_{11}$, 649.3588); 1H NMR (400 MHz, pyridine- d_5) and ^{13}C NMR (100 MHz, pyridine- d_5) data, see Tables S1–S2.

Dehydrosulphurenic acid 3-O- β -D-glucoside (9a): white amorphous powder; HR-ESI-MS: m/z 645.4007 ($[M-H]^-$, calcd. for $C_{37}H_{57}O_9$, 645.4003); 1H NMR (600 MHz, pyridine- d_5) and ^{13}C NMR (150 MHz, pyridine- d_5) data, see Tables S1–S2.

Dehydrosulphurenic acid 15-O- β -D-glucoside (9b): white amorphous powder; HR-ESI-MS: m/z 645.3989 ($[M-H]^-$, calcd. for $C_{37}H_{57}O_9$, 645.4003); 1H NMR (400 MHz, pyridine- d_5) and ^{13}C NMR (100 MHz, pyridine- d_5) data see Tables S1–S2.

Dehydrosulphurenic acid 3,15-di-O- β -D-glucoside (9c): white amorphous powder; HR-ESI-MS: m/z 807.4523 ($[M-H]^-$, calcd. for $C_{43}H_{67}O_{14}$, 807.4531); 1H NMR (400 MHz, pyridine- d_5) and ^{13}C NMR (100 MHz, pyridine- d_5) data see Tables S1–S2.

Dehydroeburicoic acid 3-O- β -D-glucoside (10a): white amorphous powder; HR-ESI-MS: m/z 629.4036 ($[M-H]^-$, calcd. for $C_{37}H_{57}O_8$, 629.4053); 1H NMR (600 MHz, pyridine- d_5) and ^{13}C NMR (150 MHz, pyridine- d_5) data see Tables S1–S2.

6. Inhibition activities against COX-2

Compounds **1–7** and **1a–7a** at 40 μ M were evaluated. The positive control was celecoxib at 100 nM. The experimental procedure was according to the manufacturer's instructions, using human COX-2 inhibitor screening kit.

7. Lipopolysaccharide (LPS)-induced acute lung injury (ALI) mice model

Male BALB/c mice (20 g) were purchased from the Experimental Animal Center of Peking University Health Science Center (Beijing, China). The mice were treated with 2 mg/kg LPS or PBS. In the meantime, the drugs were suspended in 0.5% CMC–Na solution, and were given to the mice intragastrically. The mice were divided into six groups: (1) PBS + 0.5% CMC–Na solution (blank), (2) LPS + 0.5% CMC–Na solution (model), (3) LPS + 10 mg/kg of **4a** (**4a-L**), (4) LPS + 20 mg/kg of **4a** (**4a-H**), (5) LPS + 10 mg/kg of **4** (**4-L**), (6) LPS + 20 mg/kg of **4** (**4-H**). Each group had three mice. After 24 h, the mice were sacrificed and blood and lung tissue samples were collected.

8. Pathological analysis

The lung tissues were fixed with 4% paraformaldehyde, embedded in paraffin, and cut into 5- μ m sections. The sections were stained with H&E to demonstrate the histological structure of testes in blank, model, and compounds-treated mice. Images were taken using WISLEAP (WS-10).

9. Immunohistochemistry (IHC)

IHC experiments were carried out as described previously.^[3] Briefly, paraffin embedded lung tissues were sectioned into 5- μ m sections, and serial tissue sections were incubated for 2 h with primary antibodies (Abcam, IL-1 β , 1:250; IL-6, 1:50), then secondary staining was performed with HRP-conjugated goat anti-mouse IgG (1:200).

DAB was incubated for 2 min. Finally, the reaction was terminated, and the sections were stained using hematoxylin. Images were taken using WISLEAP (WS-10).

Table S1. ¹H NMR Spectroscopic Data (in pyridine-*d*₅) for Compounds **1a–7a**, **9a–9c**, and **10a** (δ in ppm, *J* in Hz).

No.	1a/2a ^d	3a/4a ^d	5a ^d	6a/7a ^d	9a ^e	9b ^d	9c ^d	10a ^e
1	1.25, m	2.43, m	1.56, m	1.97, m	2.41, m	2.30, m	1.02, m	2.38, m
	3.13, m	4.33, m	3.35, m	2.79, m	2.73, m	2.75, m	2.12, m	2.55, m
2	1.97, m	3.47, m	1.74, m	1.86, m	1.88, m	1.14, m	1.03, m	1.87, m
	2.78, m	3.62, m	2.46, m		2.35, m	1.91, m		2.34, m
3	4.09, brs			3.89 ^Δ	4.69, dd (11.6, 2.5)	3.45, t (7.6)	3.39, dd (11.8, 3.9)	3.40, dd (11.8, 3.9)
4		3.35, m		1.56, m				
5	2.22, m	2.51, m	1.76, m	2.09, m	1.27, m	1.27, m	1.23, m	1.22, m
6	2.73, m	2.43, m	2.77, m	2.24, m	2.10, m	2.17, m	2.11, m	2.09, m
	3.21, m	2.82, m	3.14, m	2.45, m				
7	4.63, t (8.4)	4.48, t (7.9)	4.69, t (8.3)	4.45 ^Δ	6.48, d (6.4)	6.90, t (6.1)	6.87, d (5.8)	5.59, d (6.2)
11					5.34, d (6.4)	5.37, d (6.3)	5.29, d (6.4)	5.32, d (6.4)
12	2.44, d (13.2)	2.46, d (13.4)	2.49, d (13.3)	4.41, s	1.40, m	2.40, m	2.40, m	2.38, m
	2.92, d (13.3)	2.95, d (13.7)	2.96, d (13.8)		1.83, m	2.66, m	2.65, m	2.54, m
14	2.72, m	3.90, m	2.69, m	3.56, m				
15	1.97, m	3.11, m	2.07, m	2.09, m	4.79, q (5.7)	4.64, q (5.2)	4.61 ^Δ	1.53, m

	2.76, m	3.92, m	2.81, m	2.79, m				1.78, m
16	1.37, m	2.49, m	1.40, m	1.43, m	2.25, m	4.42, m	4.37, m	1.46, m
	1.86, m	3.05, m	1.92, m	1.98, m	2.34, m			2.13, m
17	1.41, m	2.50, m	1.41, m	2.43, m	2.80, m	2.63, m	2.63, m	2.53, m
18	0.82, s	0.84, s	0.82, s	0.90, s	1.13, s	1.14, s	1.12, s	0.99 ^Δ
19	2.08, s	1.56, s	2.00, s	1.56, s	1.03 ^Δ	1.10, s	1.02 ^Δ	0.99 ^Δ
20	1.33, m	2.43, m	1.29, m	1.45, m	2.65, m	2.63, m	2.62, m	2.64, m
21	0.85, d (6.0)	0.87, d (5.3)	0.88, d (5.8)	1.06, d (6.3)				
22	1.26, m	3.08, m	2.47, m	1.34, m	2.31, m	2.26, m	2.24, m	1.53, m
	1.76, m	3.95, m	3.24, m	1.83, m	2.43, m	2.34, m	2.35, m	1.78, m
23	2.19, m	3.30, m	2.18, m	1.91, m	1.94, m	1.90, m	1.91, m	1.92, m
	2.39, m	3.55, m	2.38, m	2.79, m	2.09, m			2.07, m
25	3.47, q (6.9)	4.58, q (6.7)	3.46, q (6.8)	3.45, q (7.0)	2.26, m	2.22, m	2.23, m	2.28, m
26					1.01 ^Δ	1.00 ^Δ	1.01 ^Δ	1.03 ^Δ
27	1.51, d (7.0)	1.52, d (7.1)	1.52, d (7.0)	1.51, d (7.0)	1.01 ^Δ	1.00 ^Δ	1.01 ^Δ	1.03 ^Δ
28	5.06 ^Δ	5.07, s	5.07, s	5.04, s	4.87, s	4.83, s	4.83, s	4.90, s
	5.23, s	5.23, s	5.24, s	5.23, s	4.91, s	4.87, s	4.87, s	4.94, s
29	1.84, s	1.23, d (6.5)	1.68, s	1.26, d (6.7)	1.30, s	1.06, m	1.17, s	1.32 ^Δ

30					1.09, s	1.09, s	1.05, s	1.10, s
31					1.48, s	1.40, s	1.40, s	1.09, s
1'	5.05 ^d	5.01, d (7.8)	5.09, d (7.8)	5.00, d (7.7)	4.93, d (7.7)	5.08, d (7.8)	4.92, d (7.7)	4.93, d (7.8)
2'	3.99, m	4.06, m	4.02, m	4.06, m	4.05, m	4.10, m	4.04, m	4.05, m
3'	4.04, m	4.02, m	4.06, m	4.00, m	4.01, m	4.03, m	4.01, m	4.01, m
4'	4.19, m	4.28, m	4.18, m	4.29, m	4.25, m	4.33, m	4.25, m	4.26, m
5'	4.26, m	4.48, m	4.27, m	4.46, m	4.25, m	4.32, m	4.25, m	4.26, m
6'	4.30, m	4.42, m	4.30, m	4.45, m	4.43, m	4.42, m	4.43, m	4.43, m
	4.55, m	4.58, m	4.58, m	4.56, m	4.58, m	4.55, m	4.56, m	4.59, m
1"							5.06, d (7.8)	
2"							4.10, m	
3"							4.02, m	
4"							4.32, m	
5"							4.33, m	
6"							4.37, m	
							4.56, m	

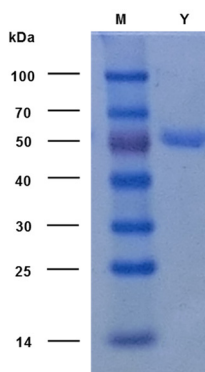
^d Recorded at 400 MHz. ^e Recorded at 600 MHz. ^Δ overlapped signals.

Table S2. ^{13}C NMR Spectroscopic Data (in pyridine- d_5) for Compounds **1a–7a**, **9a–9c**, and **10a** (δ in ppm)

No.	1a/2a ^d	3a/4a ^d	5a ^d	6a/7a ^d	9a ^e	9b ^d	9c ^d	10a ^e
1	30.0, CH ₂	36.6, CH ₂	37.3, CH ₂	29.9, CH ₂	37.2, CH ₂	37.8, CH ₂	37.7, CH ₂	36.3, CH ₂
2	27.0, CH ₂	38.5, CH ₂	35.1, CH ₂	30.9, CH ₂	27.5, CH ₂	29.0, CH ₂	27.5, CH ₂	27.5, CH ₂
3	74.9, CH	211.8, C	213.9, C	70.5, CH	89.2, CH	78.4, CH	89.3, CH	89.2, C
4	74.4, C	44.8, CH	77.0, C	36.2, CH	39.8, C	39.6, C	39.8, C	39.8, C
5	43.7, CH	49.1, CH	51.4, CH	40.5, CH	50.2, CH	49.9, CH	50.0, CH	50.2, CH
6	29.6, CH ₂	34.9, CH ₂	29.9, CH ₂	32.5, CH ₂	23.6, CH ₂	24.1, CH ₂	23.8, CH ₂	23.6, CH ₂
7	79.7, CH	78.6, CH	79.4, CH	79.3, CH	122.5, CH	123.8, CH	123.4, CH	121.5, CH
8	151.4, C	153.1, C	152.7, C	151.5, C	142.3, C	141.4, C	141.4, C	143.2, C
9	146.7, C	143.7, C	144.7, C	144.1, C	147.2, C	147.4, C	147.1, C	146.8, C
10	38.6, C	37.3, C	37.9, C	37.5, C	37.9, C	38.3, C	37.8, C	37.8, C
11	201.9, C	201.8, C	201.7, C	203.2, C	116.7, CH	116.0, CH	116.1, CH	117.0, CH
12	59.0, CH ₂	58.5, CH ₂	58.9, CH ₂	81.9, CH	36.6, CH ₂	36.7, CH ₂	36.7, CH ₂	36.5, CH ₂
13	48.5, C	48.6, C	48.4, C	51.2, C	45.3, C	44.6, C	44.6, C	44.6, C
14	54.3, CH	54.2, CH	54.2, CH	47.7, CH	52.9, C	53.2, C	53.2, C	50.9, C
15	25.1, CH ₂	25.0, CH ₂	25.3, CH ₂	24.9, CH ₂	74.1, CH	85.8, CH	85.9, CH	32.0, CH ₂
16	28.5, CH ₂	28.6, CH ₂	28.6, CH ₂	27.9, CH ₂	40.0, CH ₂	61.6, CH ₂	62.3, CH ₂	27.6, CH ₂
17	55.3, CH	55.2, CH	55.2, CH	46.3, CH	46.9, CH	46.9, CH	46.9, CH	48.5, CH
18	12.7, CH ₃	12.8, CH ₃	12.8, CH ₃	12.6, CH ₃	17.2, CH ₃	17.2, CH ₃	17.2, CH ₃	16.6, CH ₃
19	21.2, CH ₃	18.0, CH ₃	20.9, CH ₃	18.5, CH ₃	23.3, CH ₃	23.4, CH ₃	23.2, CH ₃	23.2, CH ₃
20	36.6, CH	36.5, CH	36.6, CH	36.8, CH	49.3, CH	49.2, CH	49.2, CH	49.5, CH
21	18.9, CH ₃	19.0, CH ₃	19.0, CH ₃	18.4, CH ₃	179.1, C	179.1, C	179.1, C	178.9, C
22	34.9, CH ₂	33.4, CH ₂	34.9, CH ₂	35.3, CH ₂	33.1, CH ₂	33.0, CH ₂	33.0, CH ₂	33.1, CH ₂
23	32.1, CH ₂	32.3, CH ₂	32.2, CH ₂	32.4, CH ₂	32.2, CH ₂	32.1, CH ₂	32.1, CH ₂	32.1, CH ₂

24	150.8, C	150.9, C	150.8, C	151.3, C	156.2, C	155.9, C	155.9, C	156.2, C
25	47.1, CH	47.0, CH	47.2, CH	47.7, CH	34.6, CH	34.5, CH	34.5, CH	34.6, CH
26	177.2, C	177.5, C	177.2, C	178.0, C	22.3, CH ₃	22.2, CH ₃	22.2, CH ₃	22.3, CH ₃
27	17.5, CH ₃	17.5, CH ₃	17.6, CH ₃	17.8, CH ₃	22.4, CH ₃	22.3, CH ₃	22.4, CH ₃	22.4, CH ₃
28	110.8, CH ₂	110.8, CH ₂	110.9, CH ₂	110.4, CH ₂	107.5, CH ₂	107.5, CH ₂	107.5, CH ₂	107.4, CH ₂
29	28.3, CH ₃	12.3, CH ₃	24.1, CH ₃	17.4, CH ₃	28.7, CH ₃	29.1, CH ₃	28.6, CH ₃	28.7, CH ₃
30					17.5, CH ₃	16.9, CH ₃	17.4, CH ₃	17.5, CH ₃
31					18.7, CH ₃	19.1, CH ₃	19.1, CH ₃	26.2, CH ₃
1'	105.6, CH	106.0, CH	105.6, CH	105.9, CH	107.4, CH	106.9, CH	107.4, CH	107.4, CH
2'	76.0, CH	76.0, CH	76.0, CH	76.1, CH	76.2, CH	75.8, CH	76.1, CH	76.2, CH
3'	78.5, CH	78.9, CH	78.8, CH	78.6, CH	78.7, CH	78.7, CH	78.7, CH	78.7, CH
4'	72.8, CH	72.3, CH	72.8, CH	72.4, CH	72.2, CH	72.2, CH	72.2, CH	72.2, CH
5'	79.0, CH	79.3, CH	79.2, CH	79.2, CH	79.2, CH	79.3, CH	79.1, CH	79.1, CH
6'	63.7, CH ₂	63.4, CH ₂	63.8, CH ₂	63.5, CH ₂	63.4, CH ₂	63.3, CH ₂	63.4, CH ₂	63.4, CH ₂
1''							107.0, CH	
2''							75.8, CH	
3''							78.7, CH	
4''							72.2, CH	
5''							79.3, CH	
6''							63.3, CH ₂	

^d Recorded at 100 MHz. ^e Recorded at 150 MHz.



M, molecular mass markers; Y, purified YjiC1 protein.

Figure S1. SDS-PAGE analysis of purified YjiC1 protein.

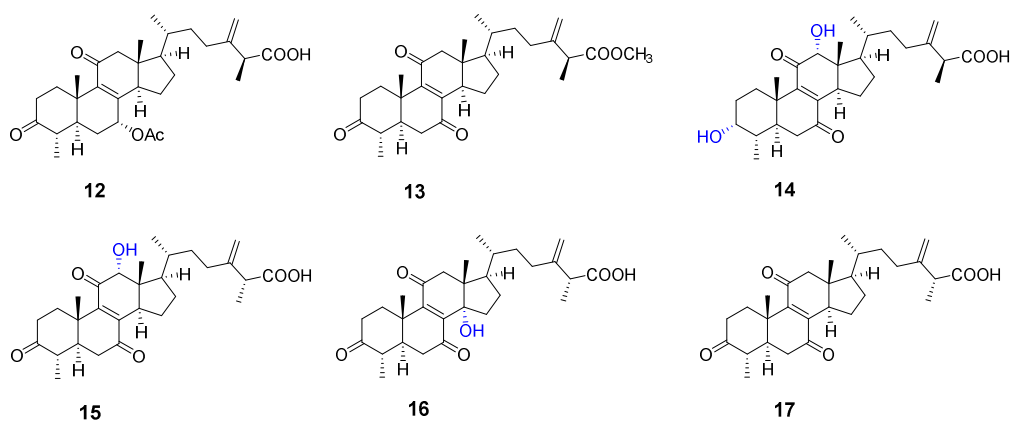


Figure S2. Structures of **12-17** that could not be catalyzed by YjiC1

(25*S*)-antcin G (**12**), (25*S*)-methyl antcin B (**13**), (25*S*)-antcin H (**14**), antcamphin I (**15**), (25*R*)-antcin D (**16**), (25*R*)-antcin B (**17**).

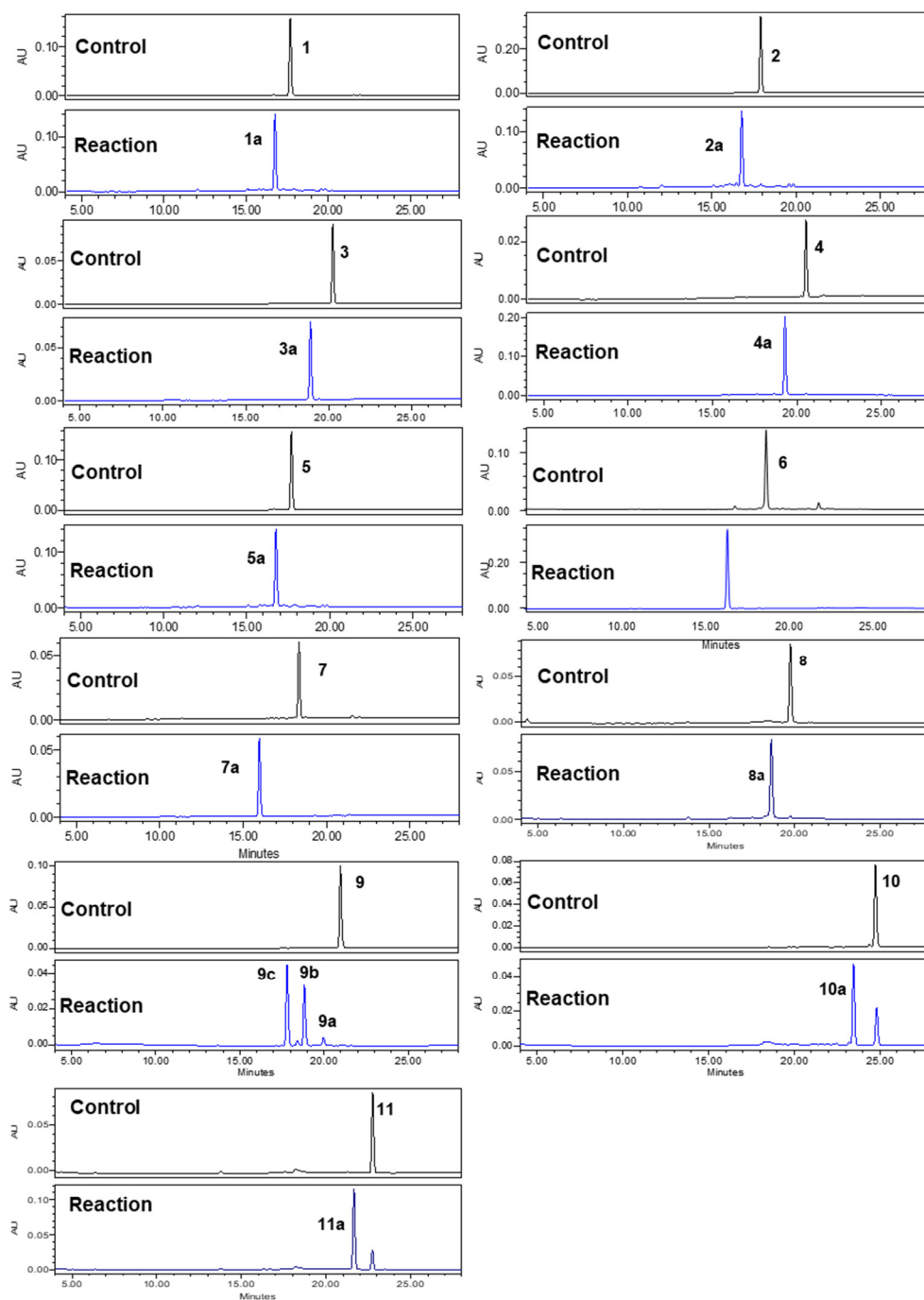


Figure S3. HPLC chromatograms of catalytic products by YjiC1 and the substrates.

UV wavelength, 254 nm.

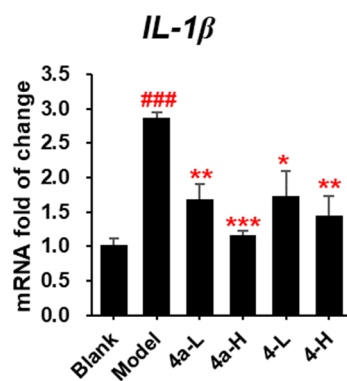


Figure S4. Effects of compounds **4a** and **4** on the mRNA expressions of IL-1 β in the mice lung tissues. Data are shown as mean \pm SEM (n = 3). ### p < 0.001 compared with the blank group; *** p < 0.001, ** p < 0.01, and * p < 0.05 compared with the model group.

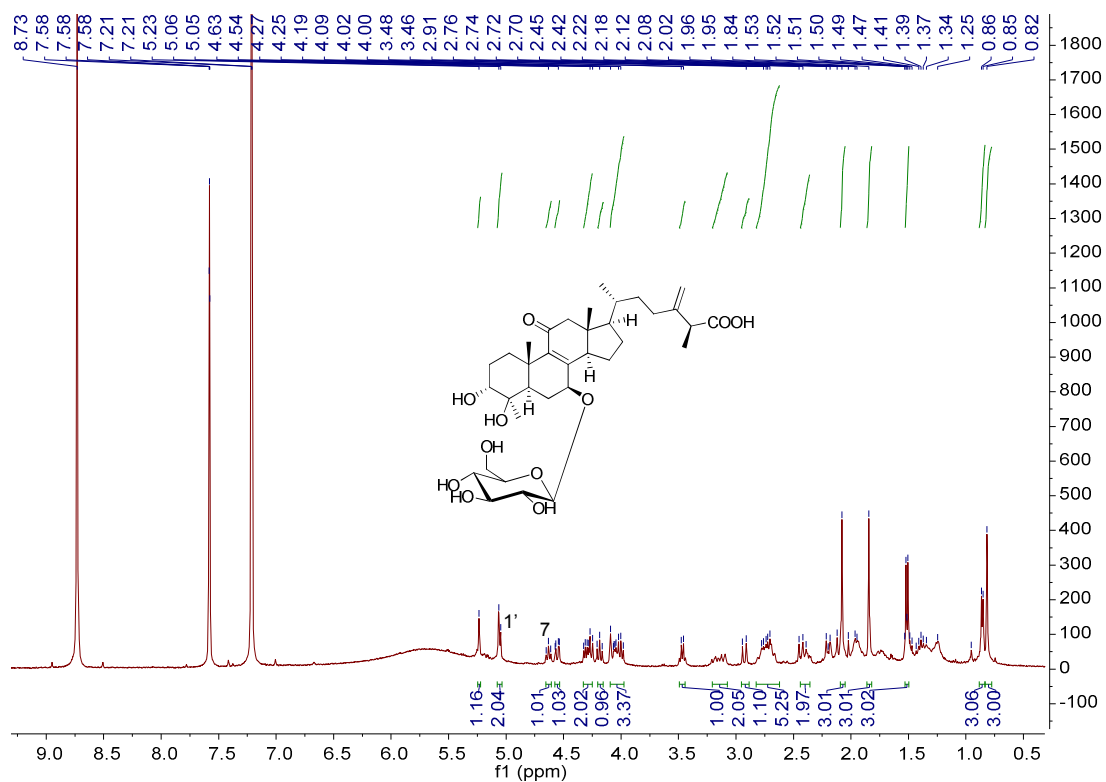


Figure S5. ^1H NMR spectrum of **1a** in pyridine- d_5 (400 MHz).

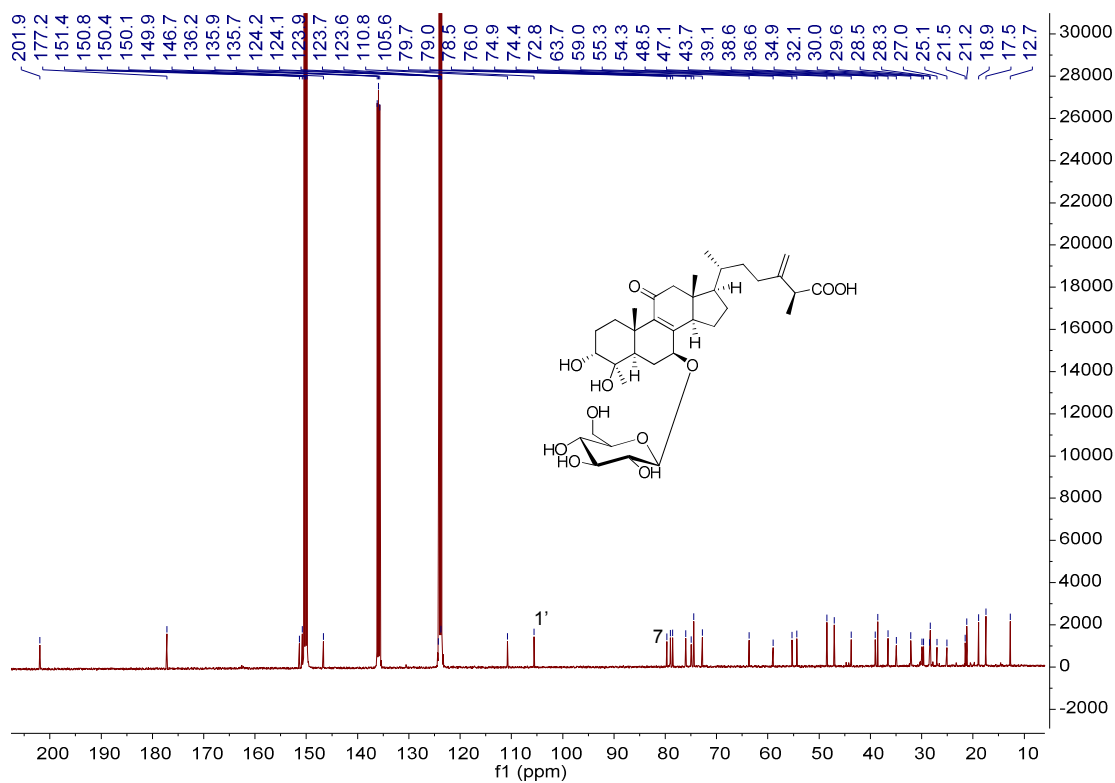


Figure S6. ^{13}C NMR spectrum of **1a** in pyridine- d_5 (100 MHz).

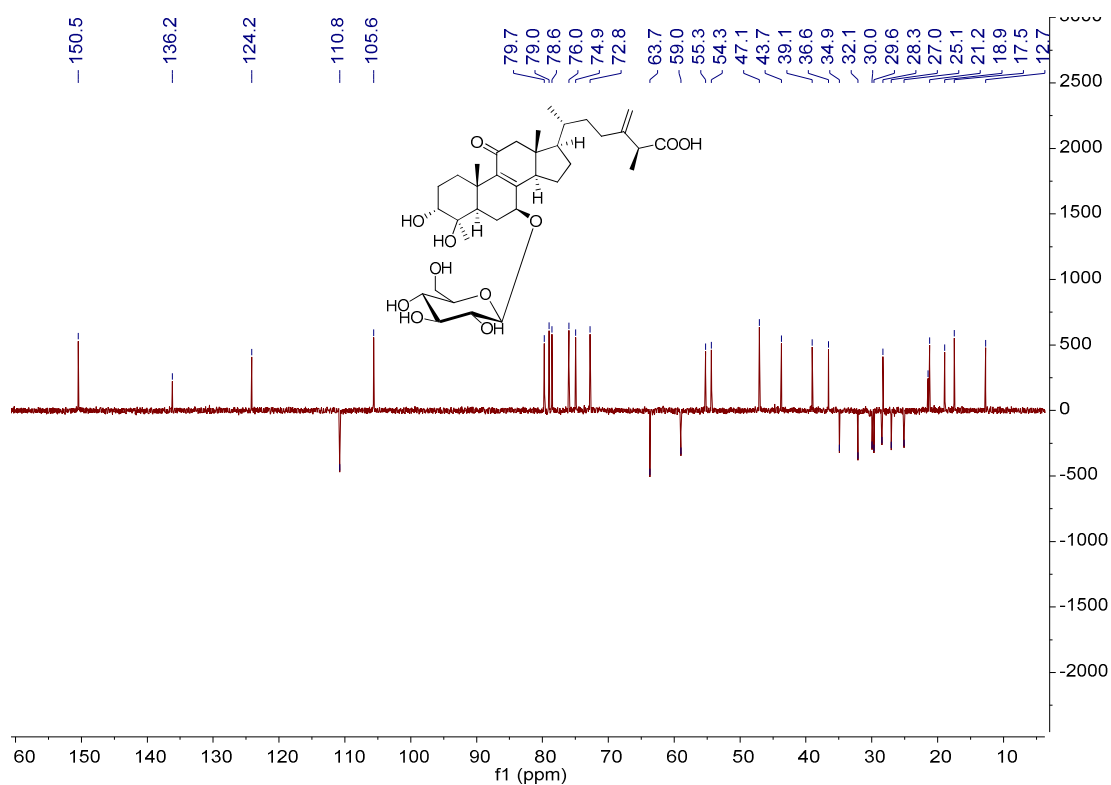


Figure S7. DEPT 135 spectrum of **1a** in pyridine-*d*₅ (100 MHz).

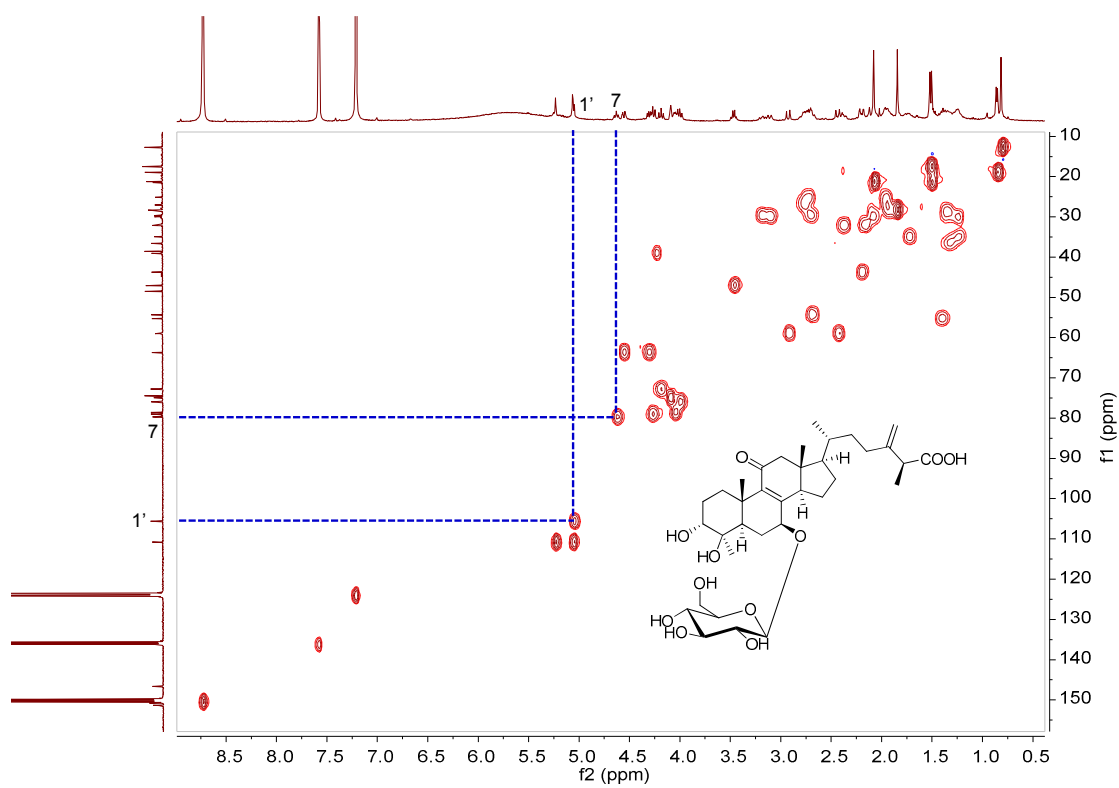


Figure S8. HSQC spectrum of **1a** in pyridine-*d*₅ (400 MHz).

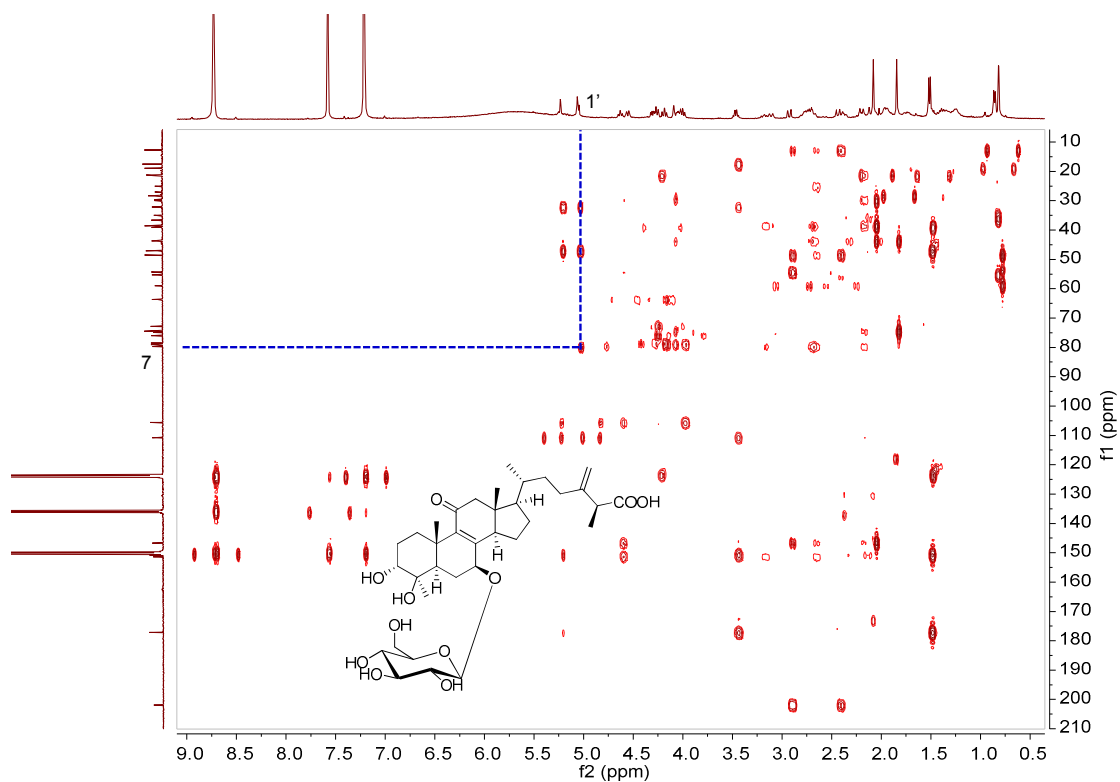


Figure S9. HMBC spectrum of **1a** in pyridine-*d*₅ (400 MHz).

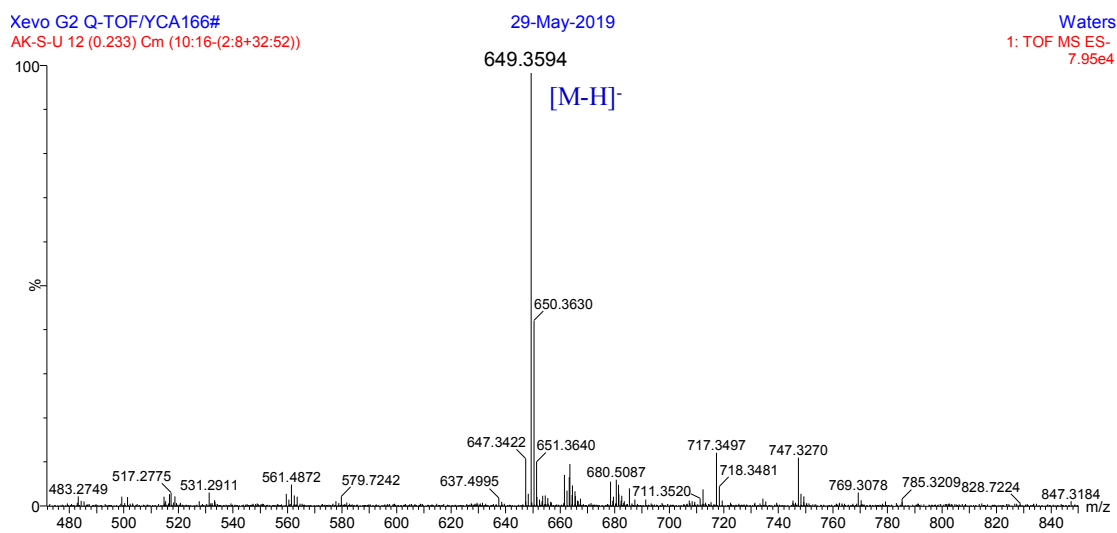


Figure S10. HR-ESI-MS spectrum of **1a**.

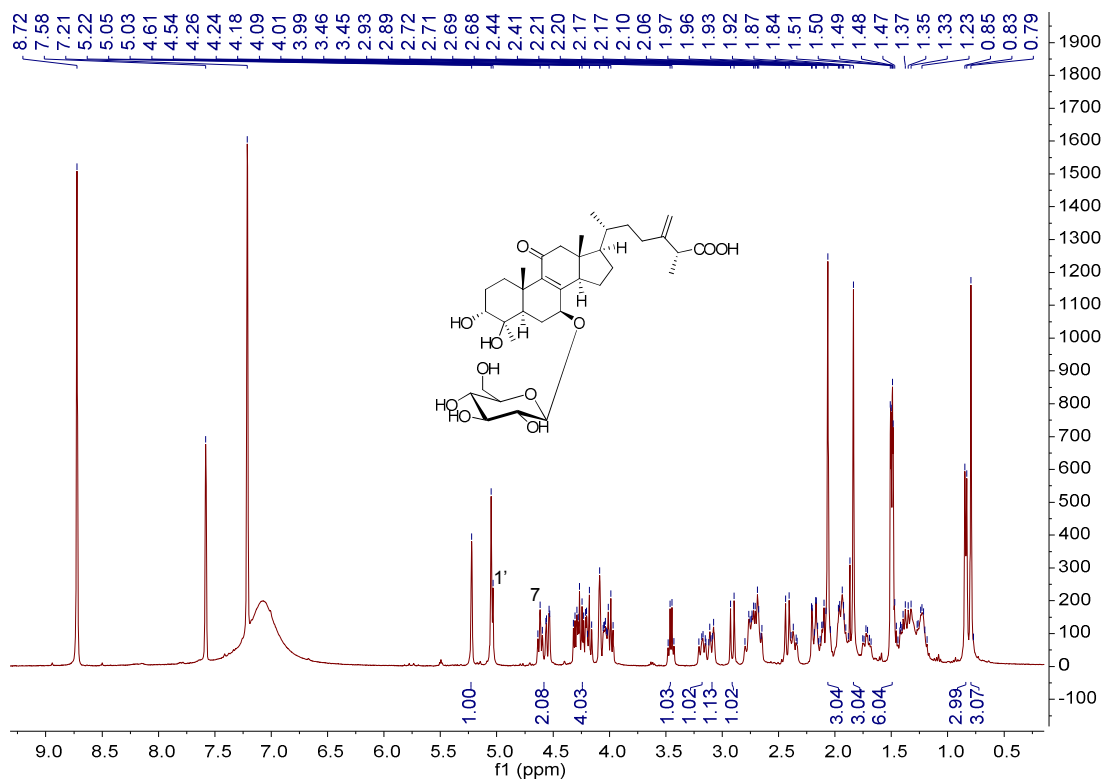


Figure S11. ^1H NMR spectrum of **2a** in pyridine- d_5 (400 MHz).

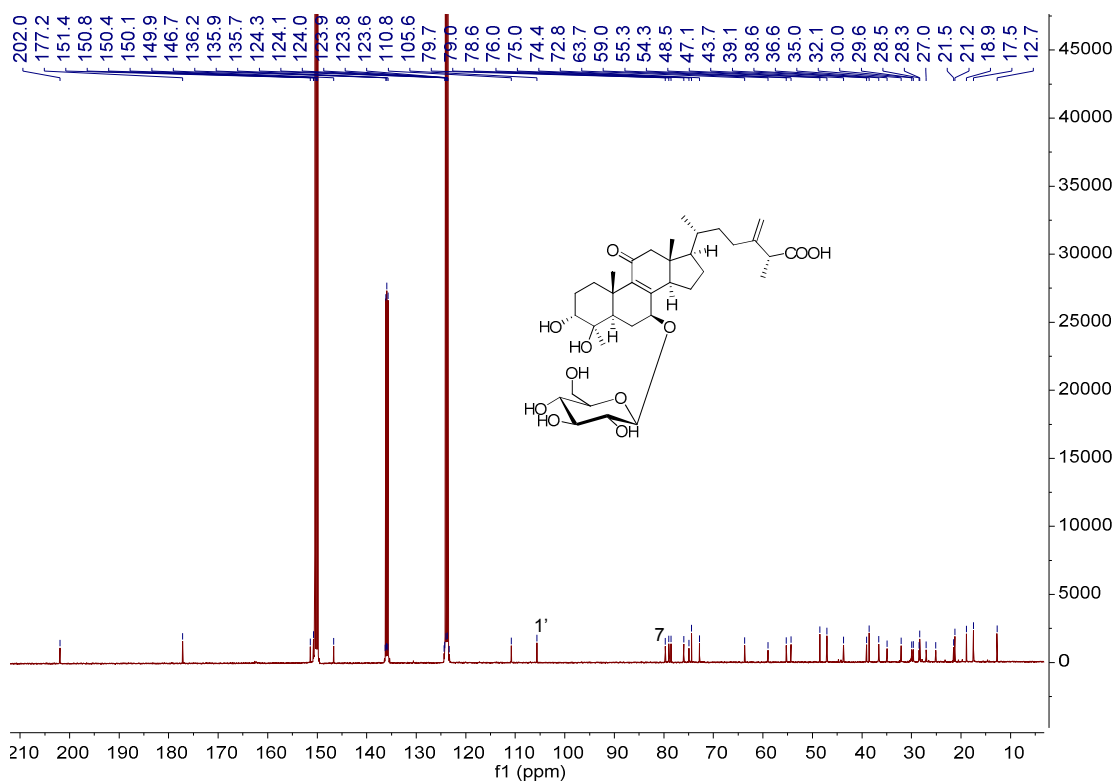


Figure S12. ^{13}C NMR spectrum of **2a** in pyridine- d_5 (100 MHz).

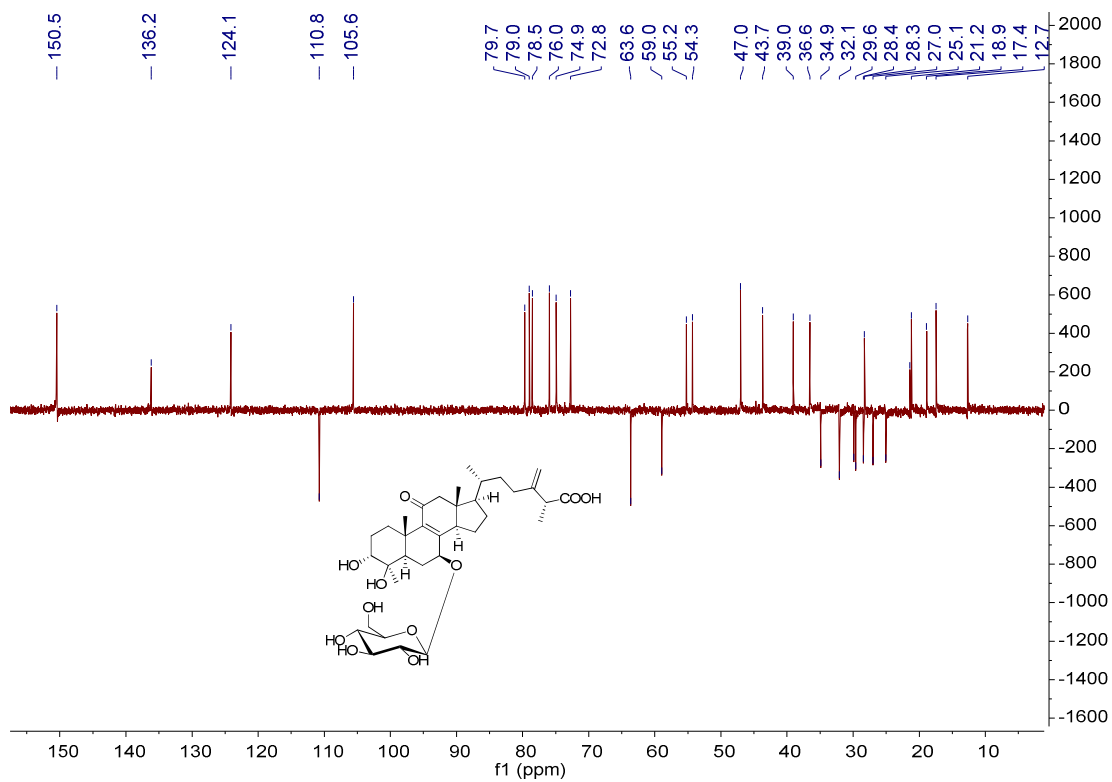


Figure S13. DEPT 135 spectrum of **2a** in pyridine-*d*₅ (100 MHz).

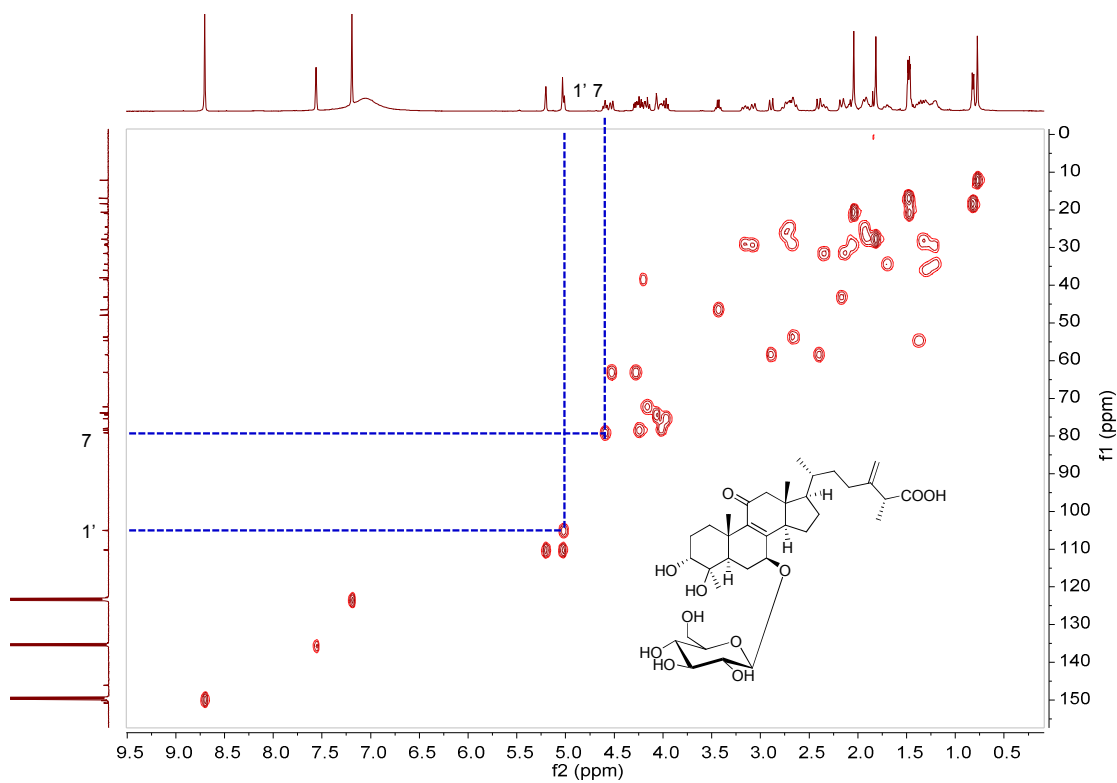


Figure S14. HSQC spectrum of **2a** in pyridine-*d*₅ (400 MHz).

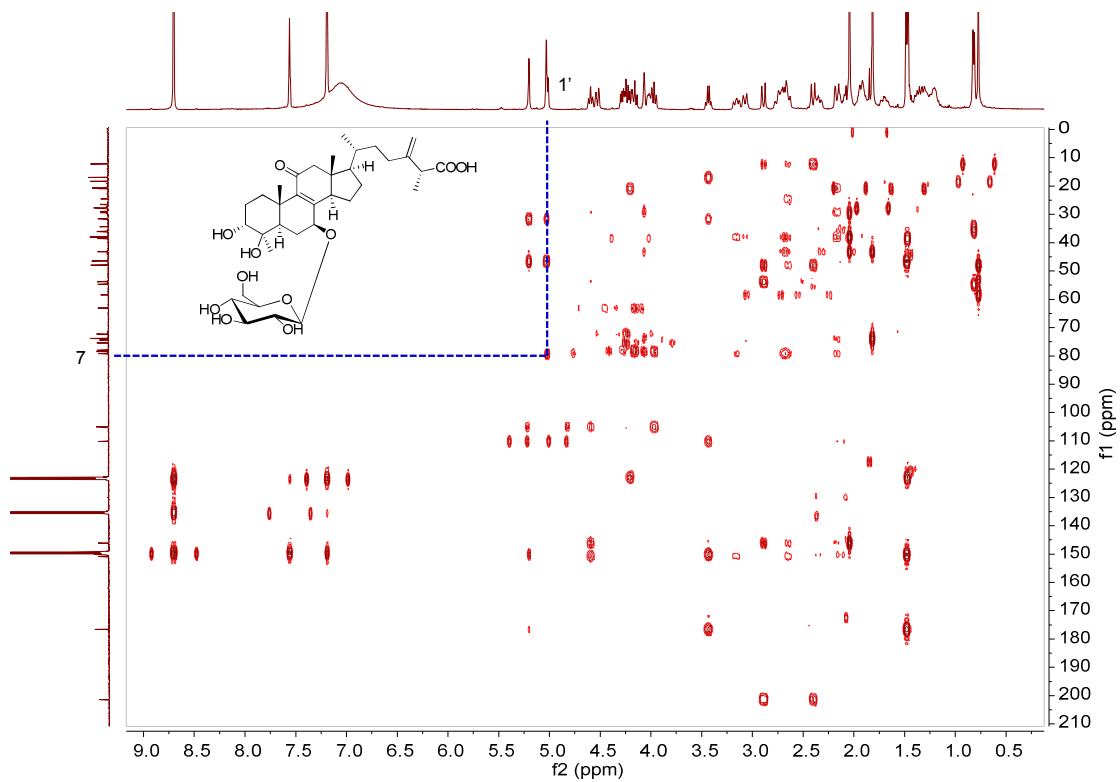


Figure S15. HMBC spectrum of **2a** in pyridine- d_5 (400 MHz).

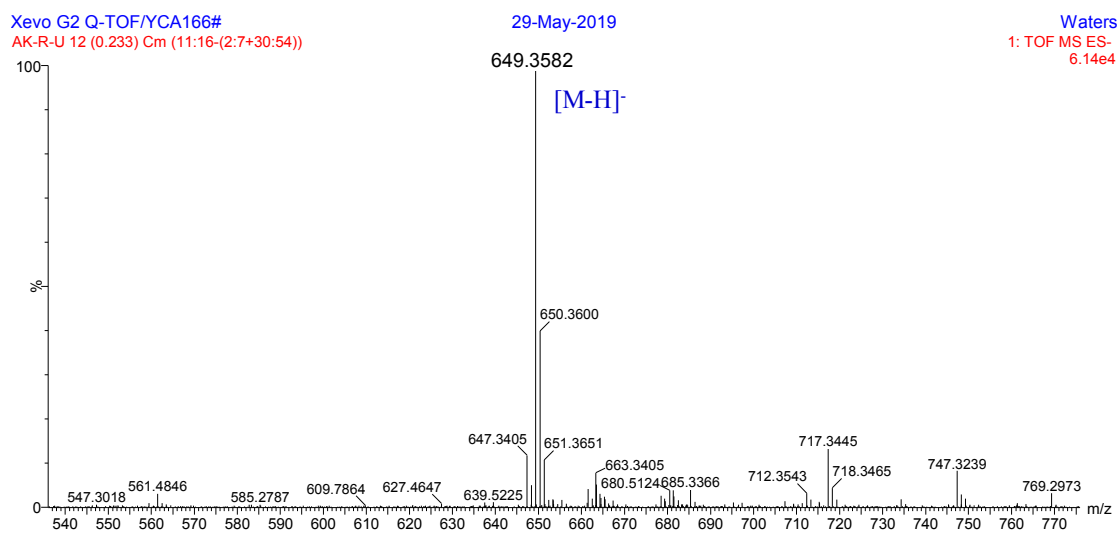


Figure S16. HR-ESI-MS spectrum of **2a**.

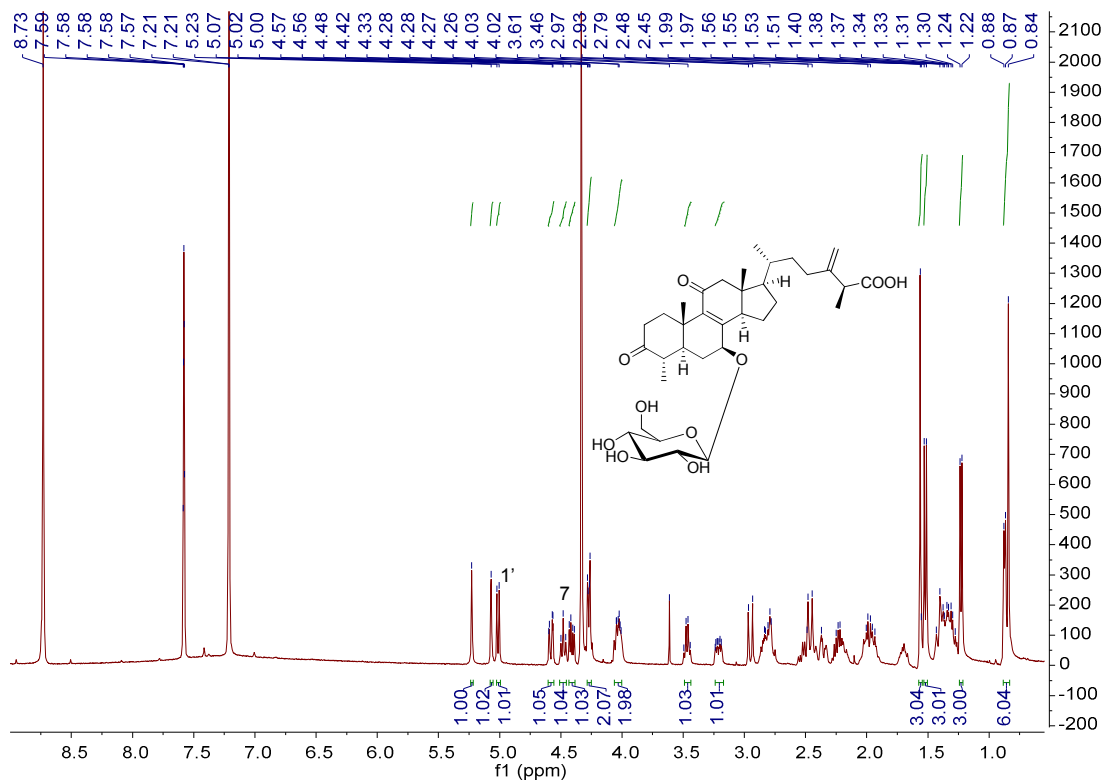


Figure S17. ^1H NMR spectrum of 3a in pyridine- d_5 (400 MHz).

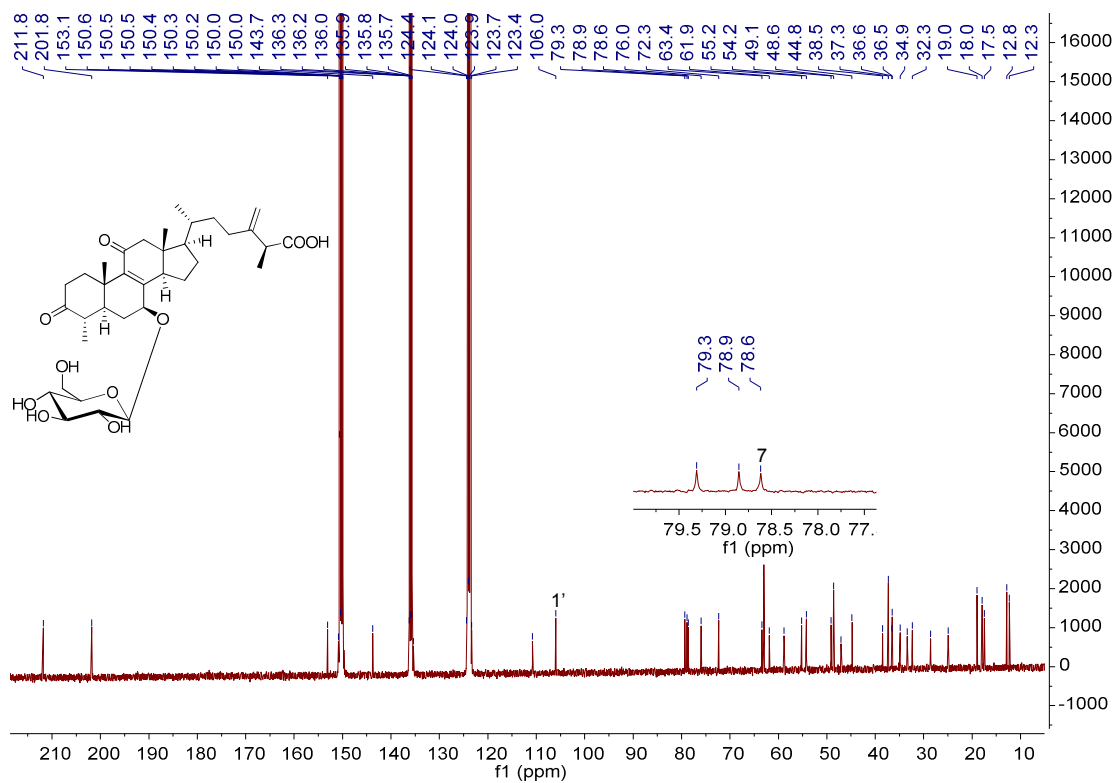


Figure S18. ^{13}C NMR spectrum of 3a in pyridine- d_5 (100 MHz).

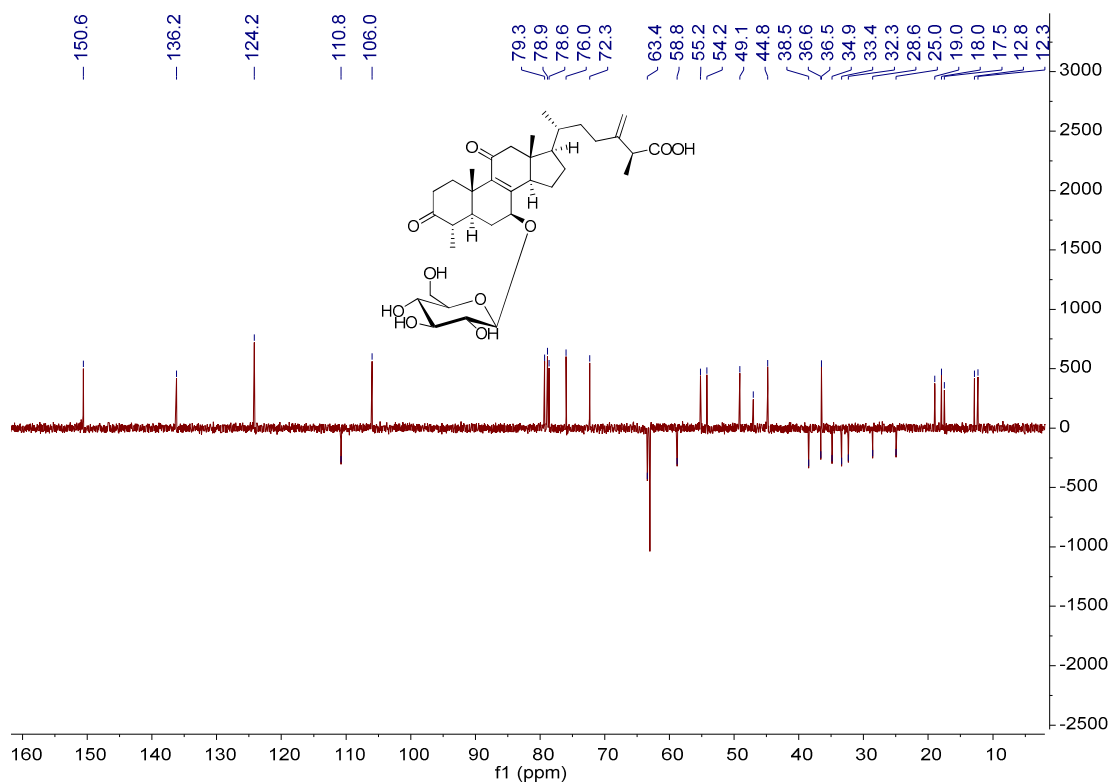


Figure S19. DEPT 135 spectrum of **3a** in pyridine-*d*₅ (100 MHz).

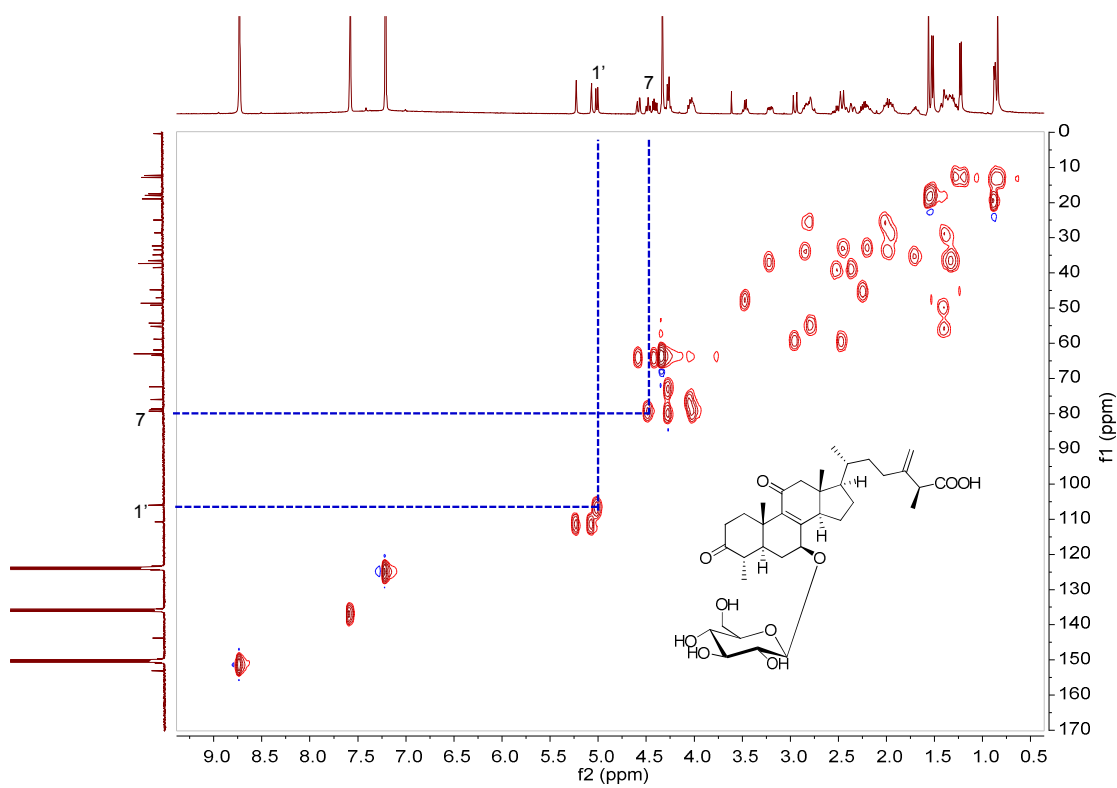


Figure S20. HSQC spectrum of **3a** in pyridine-*d*₅ (400 MHz).

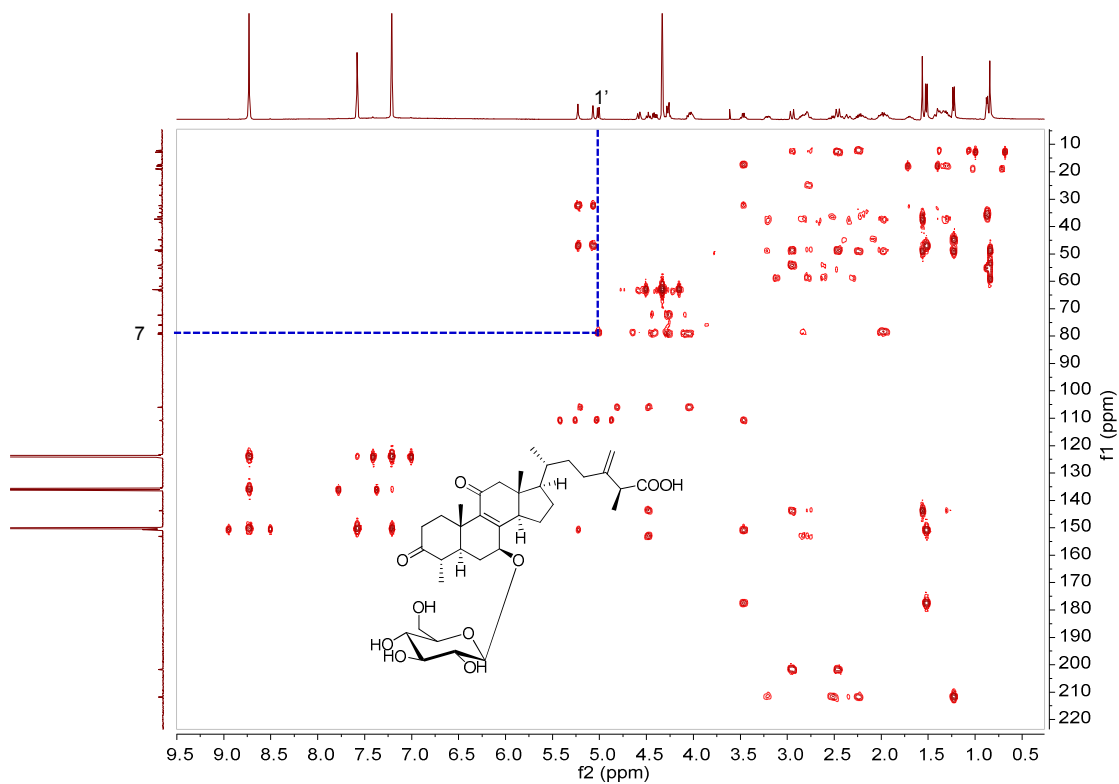


Figure S21. HMBC spectrum of **3a** in pyridine-*d*₅ (400 MHz).

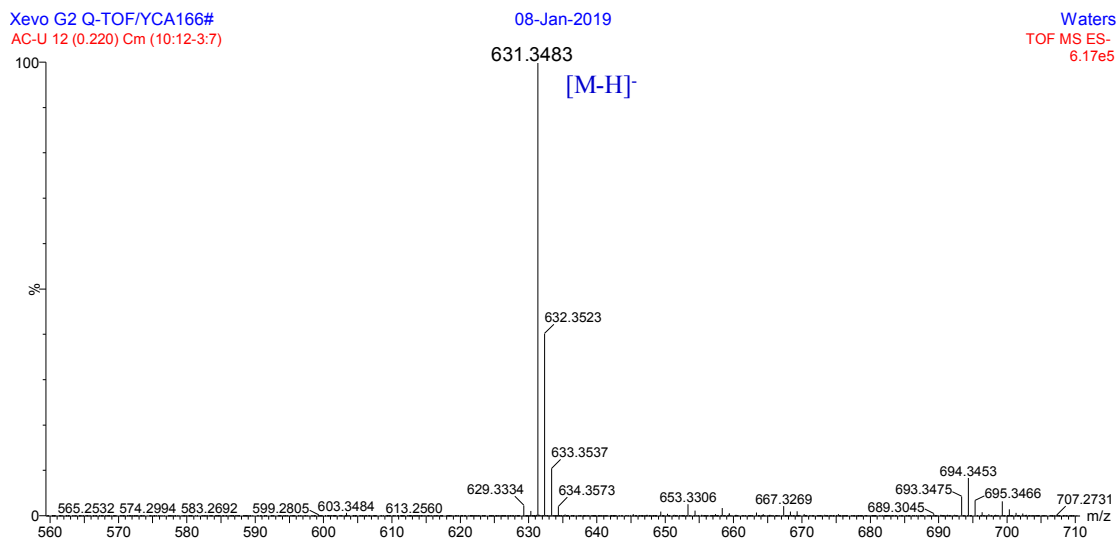


Figure S22. HR-ESI-MS spectrum of **3a**.

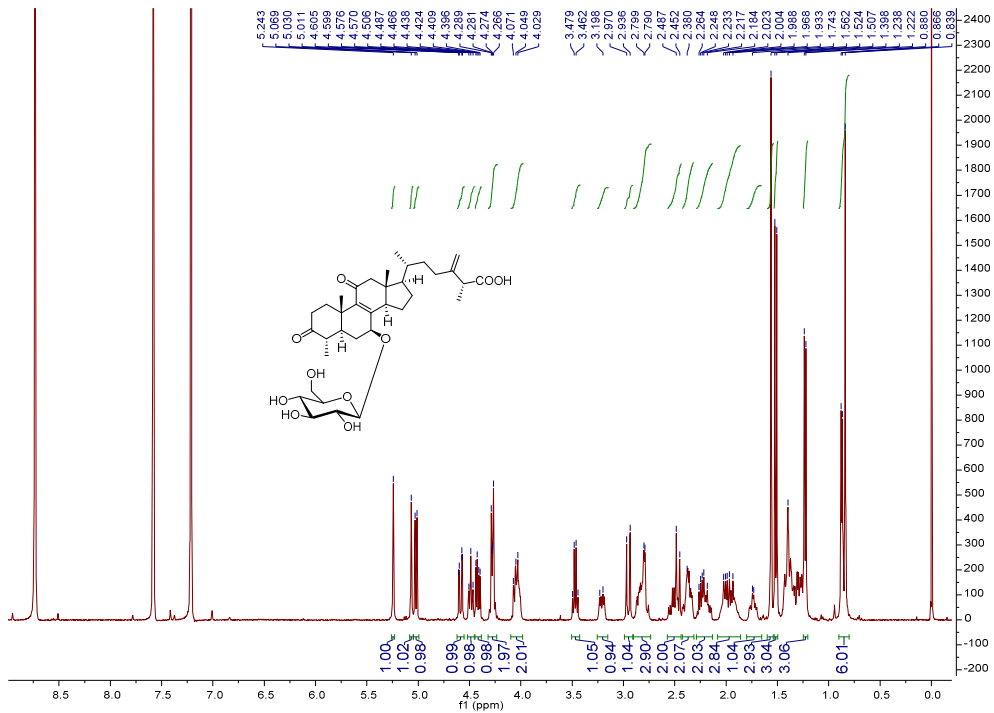


Figure S23. ^1H NMR spectrum of **4a** in pyridine- d_5 (400 MHz).

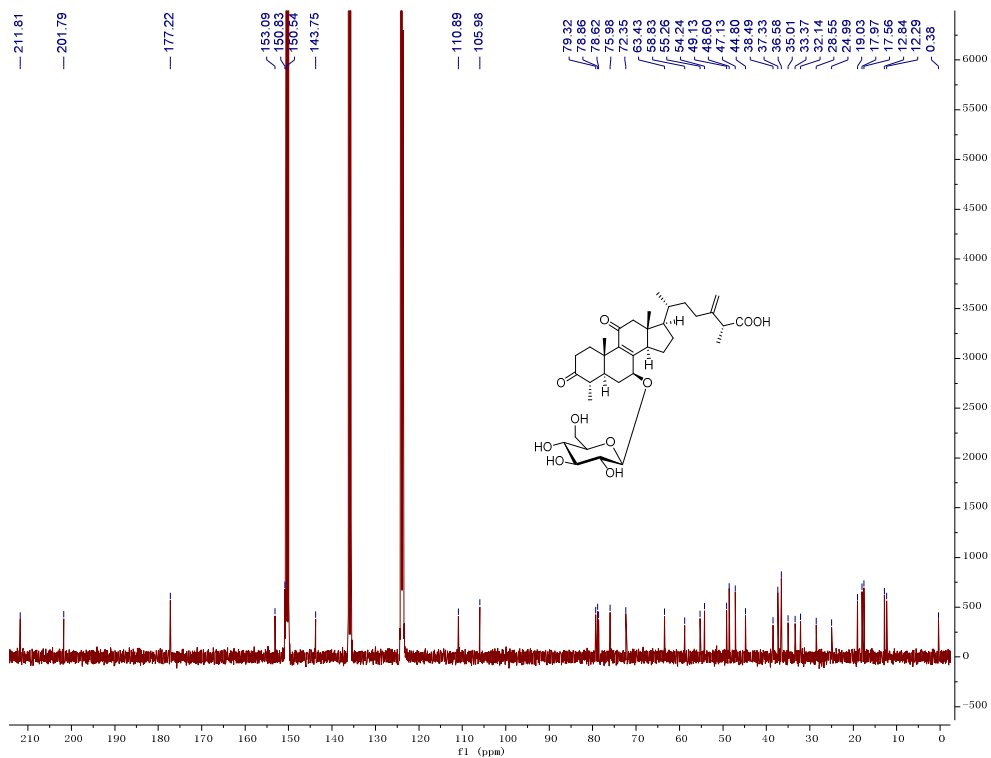


Figure S24. ^{13}C NMR spectrum of **4a** in pyridine- d_5 (100 MHz).

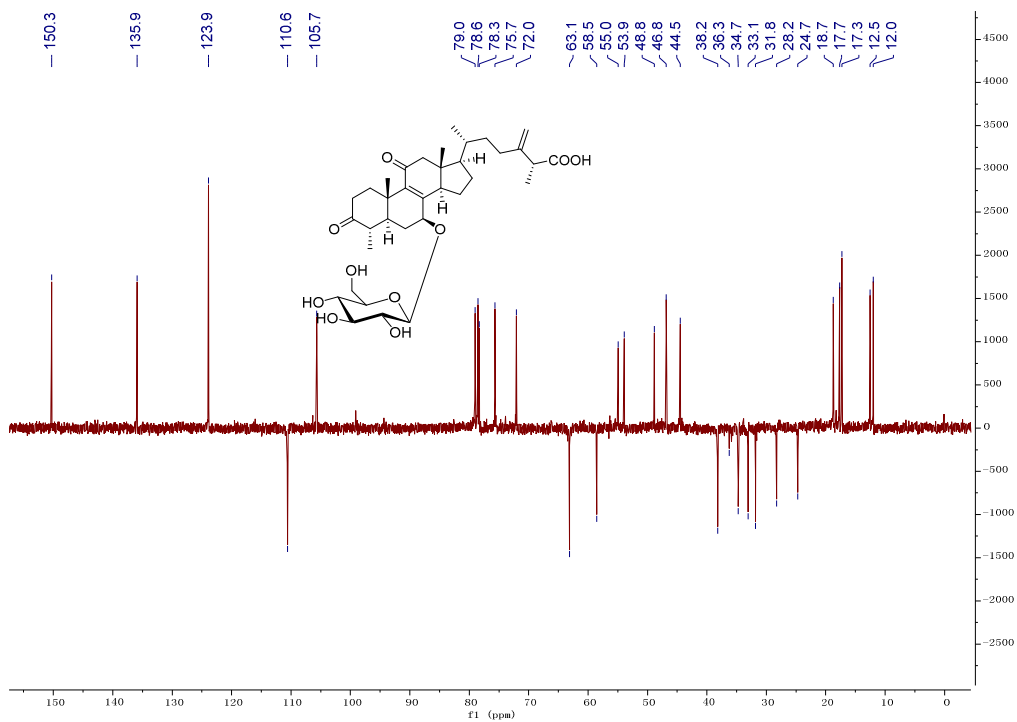


Figure S25. DEPT 135 spectrum of **4a** in pyridine-*d*₅ (400 MHz).

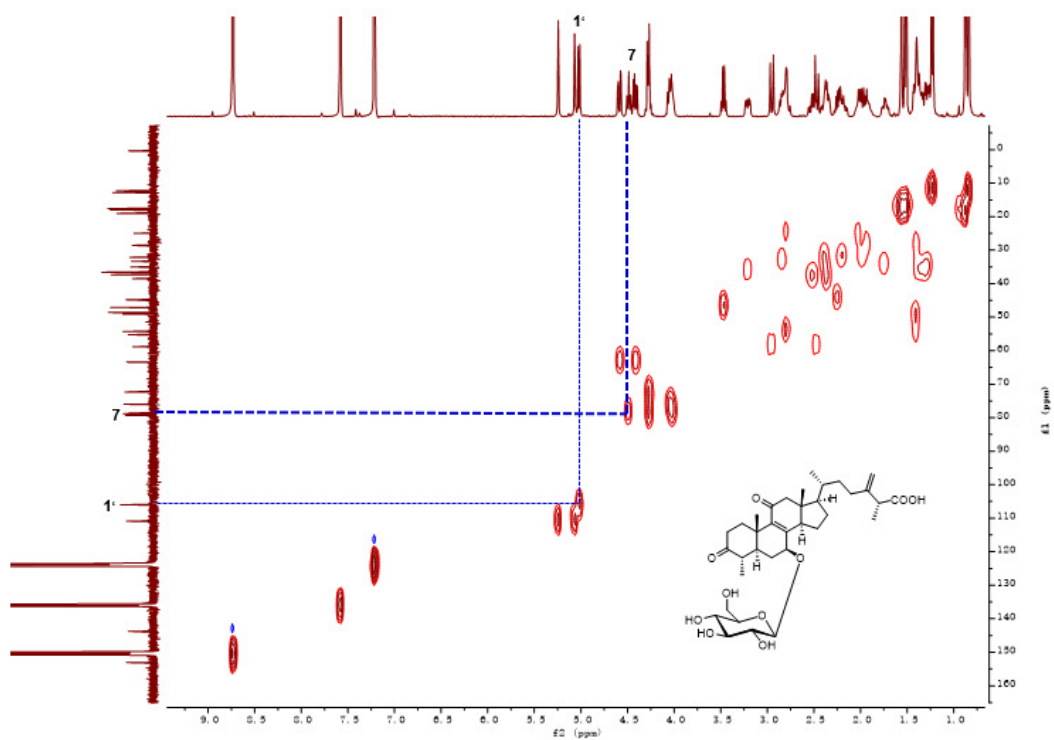


Figure S26. HSQC spectrum of **4a** in pyridine-*d*₅ (400 MHz).

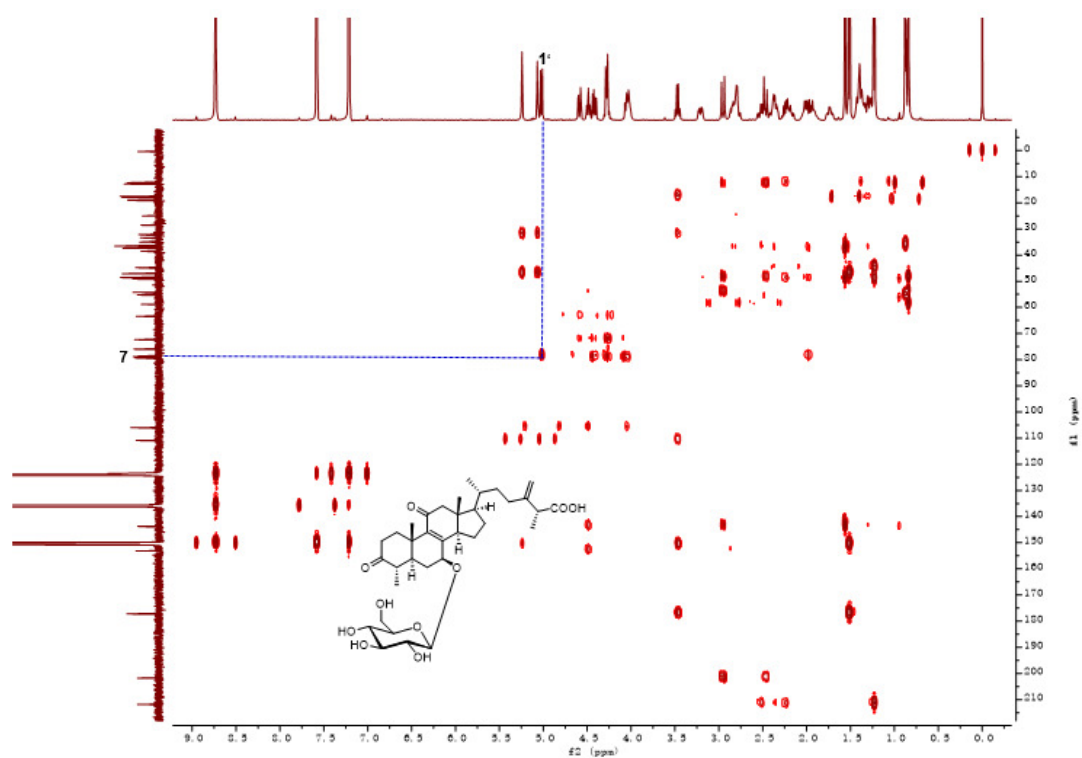


Figure S27. HMBC spectrum of **4a** in pyridine- d_5 (400 MHz).

20220214-STD-AC-R-G-PN #2493 RT: 9.09 AV: 1 NL: 5.97E8
T: FTMS - p ESI Full ms [300.0000-1000.0000]

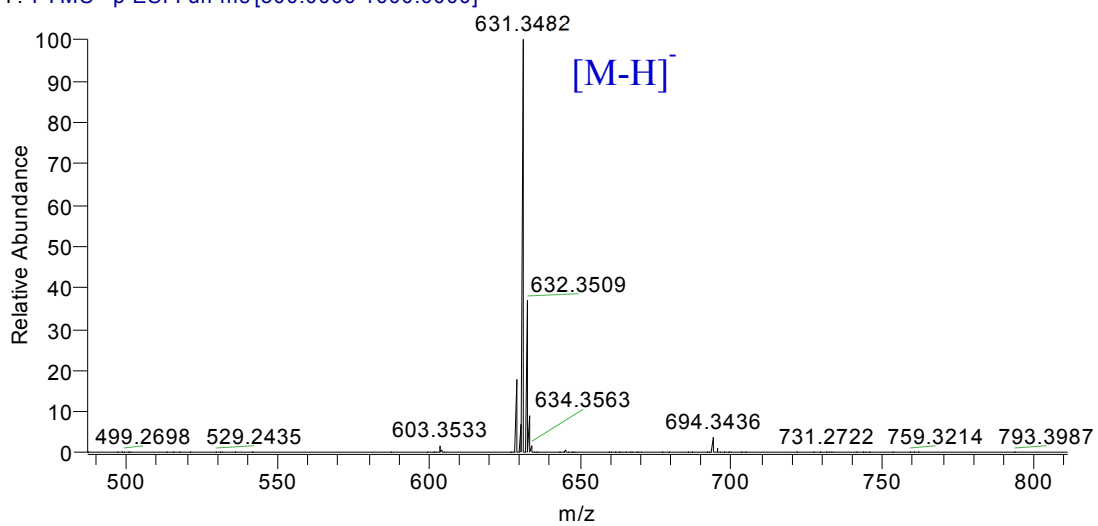


Figure S28. HR-ESI-MS spectrum of **4a**.

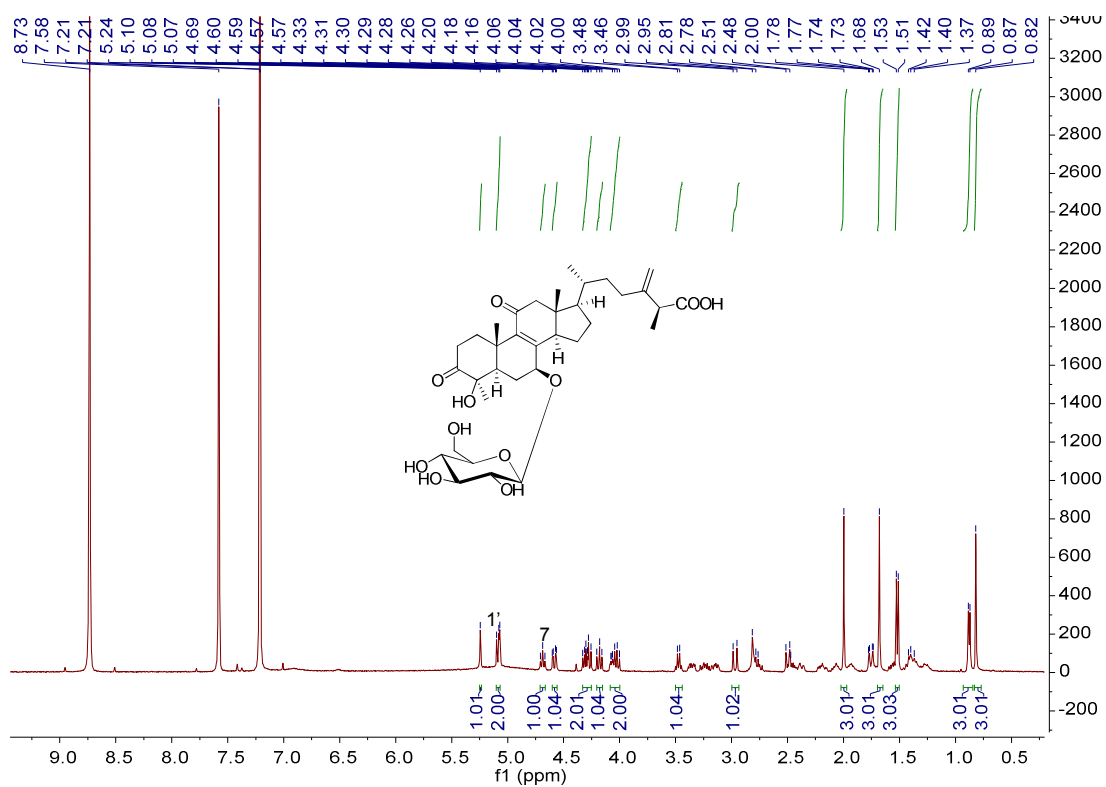


Figure S29. ^1H NMR spectrum of **5a** in pyridine- d_5 (400 MHz).

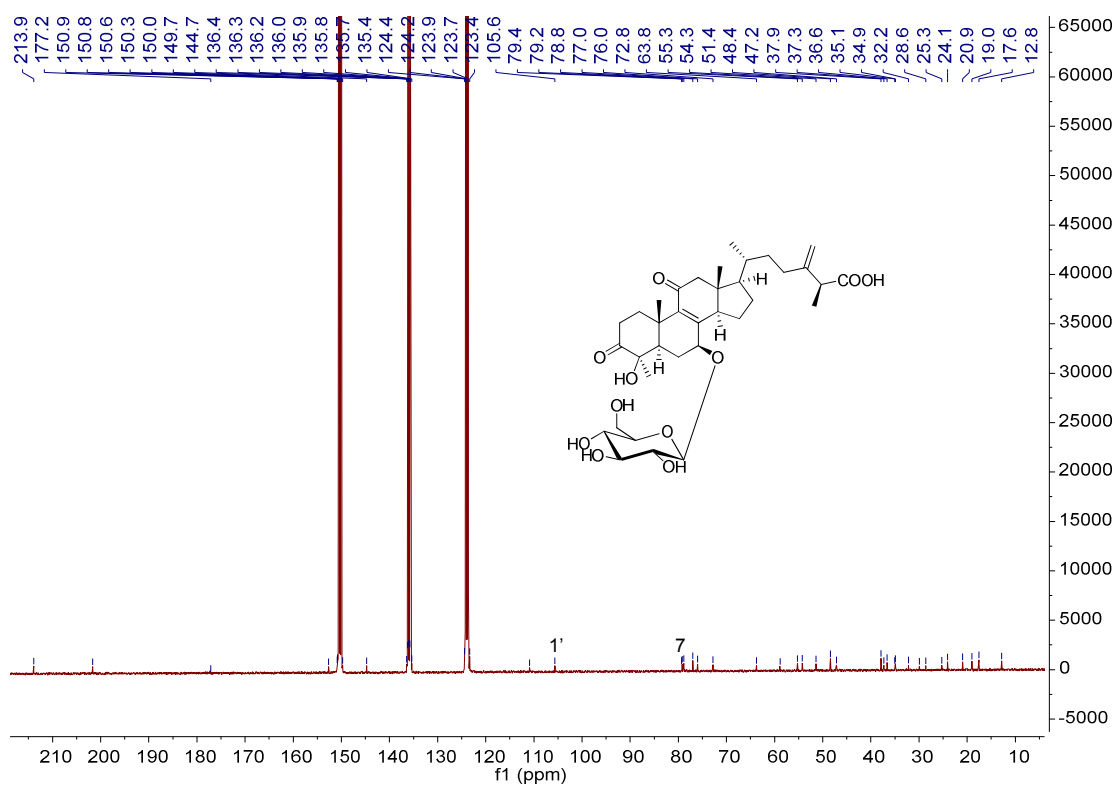


Figure S30. ^{13}C NMR spectrum of **5a** in pyridine- d_5 (100 MHz).

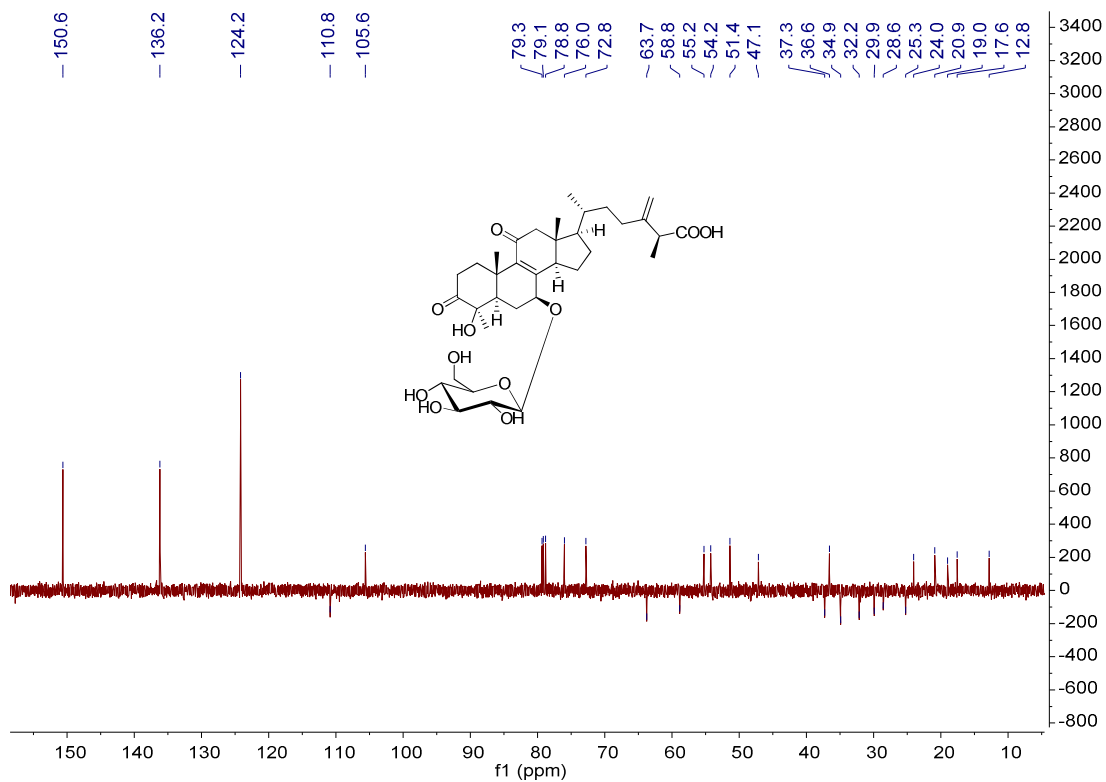


Figure S31. DEPT 135 spectrum of **5a** in pyridine-*d*₅ (100 MHz).

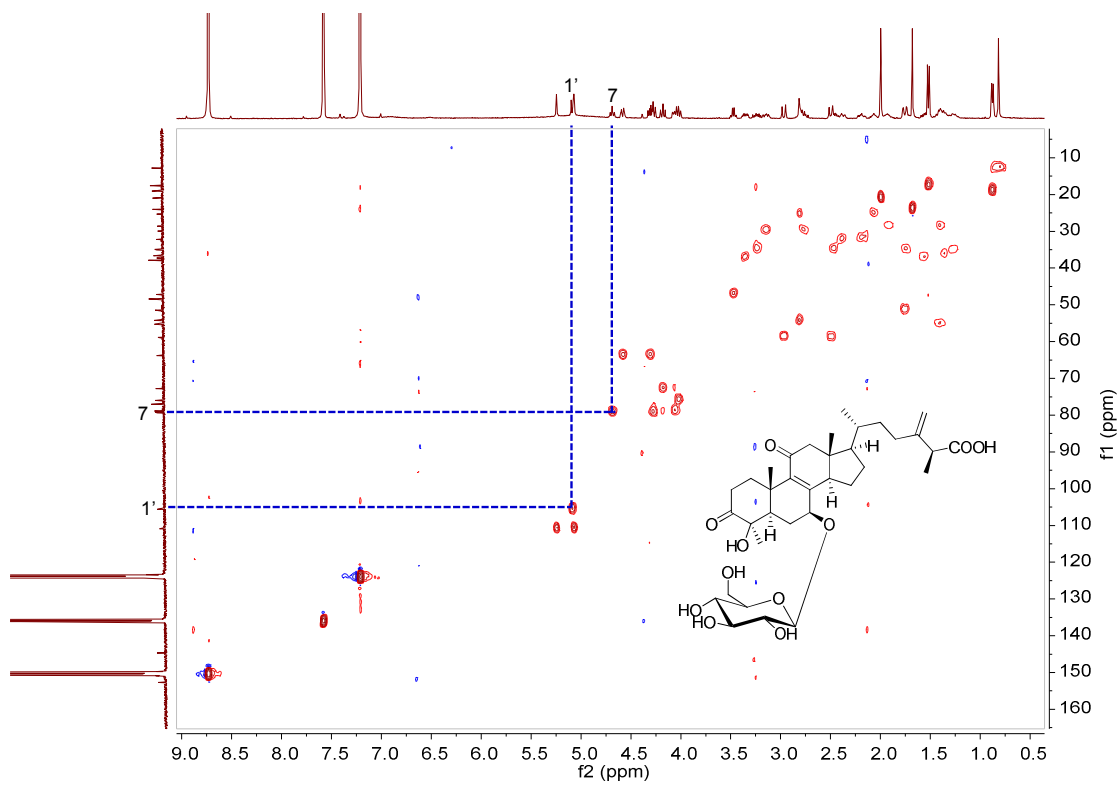


Figure S32. HSQC spectrum of **5a** in pyridine-*d*₅ (400 MHz).

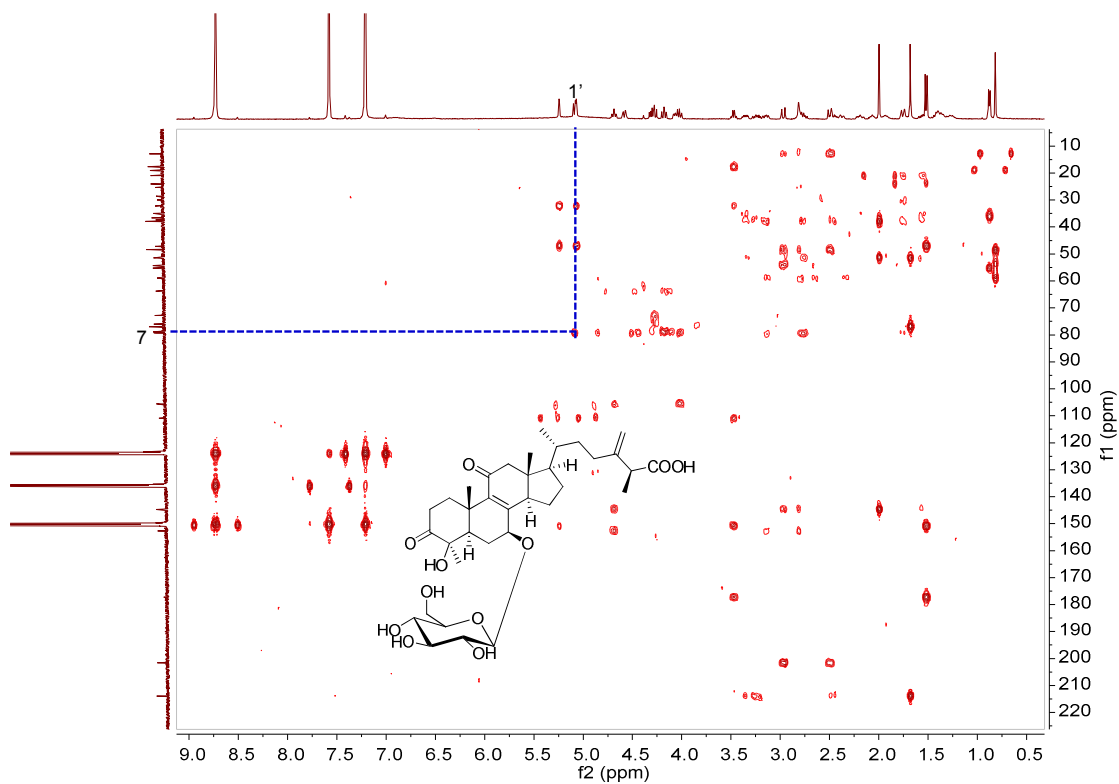


Figure S33. HMBC spectrum of **5a** in pyridine- d_5 (400 MHz).

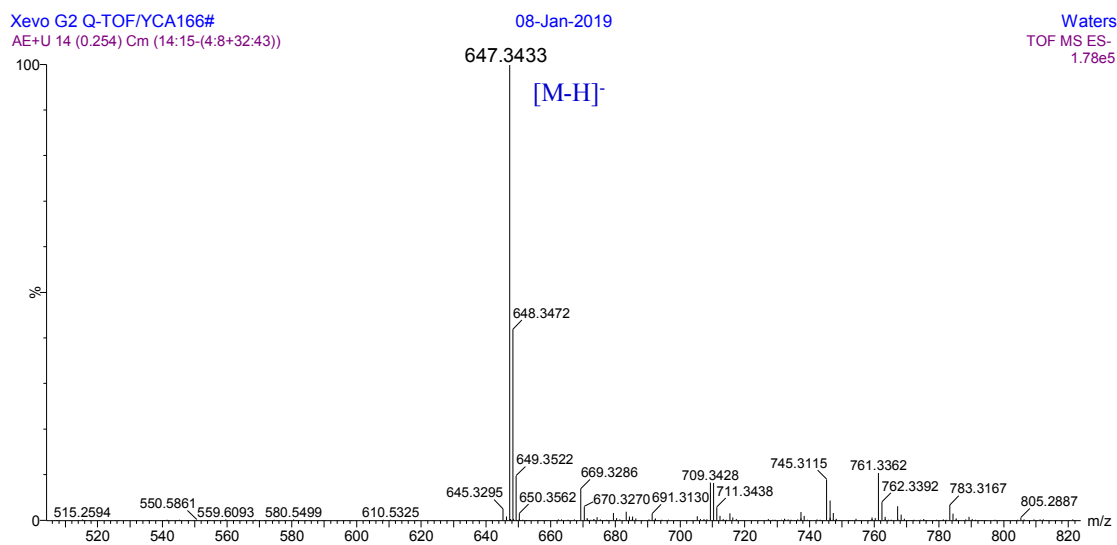
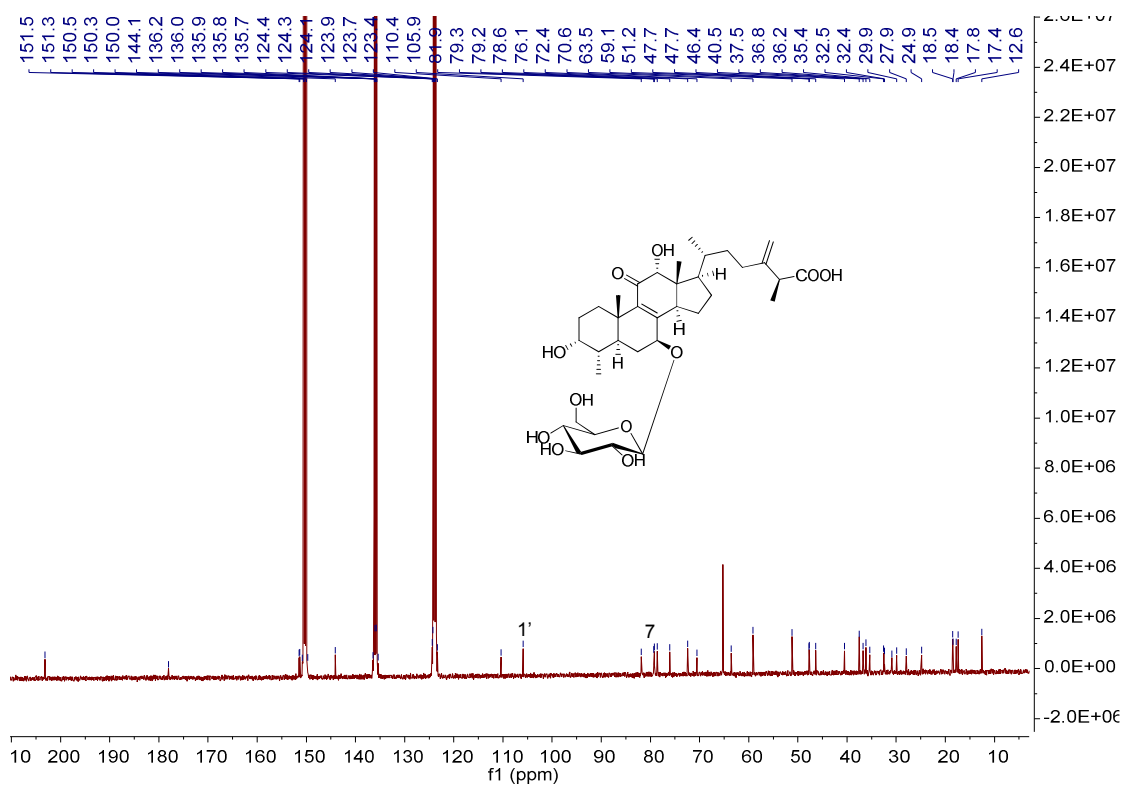
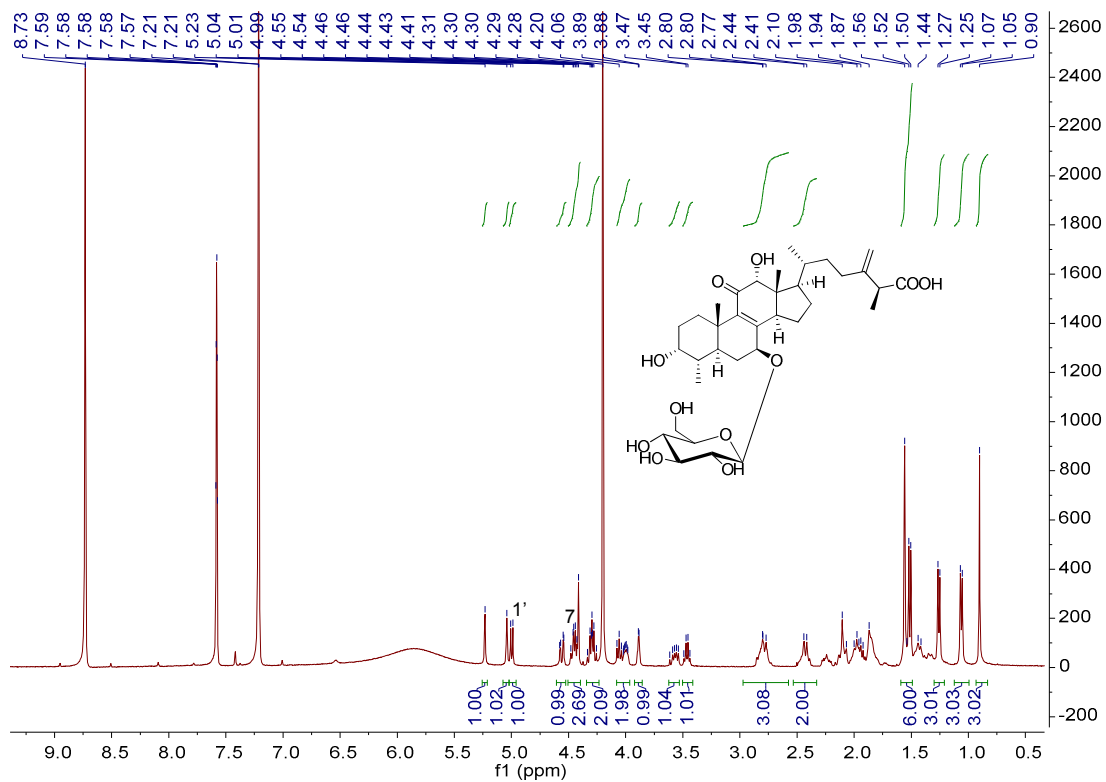


Figure S34. HR-ESI-MS spectrum of **5a**.



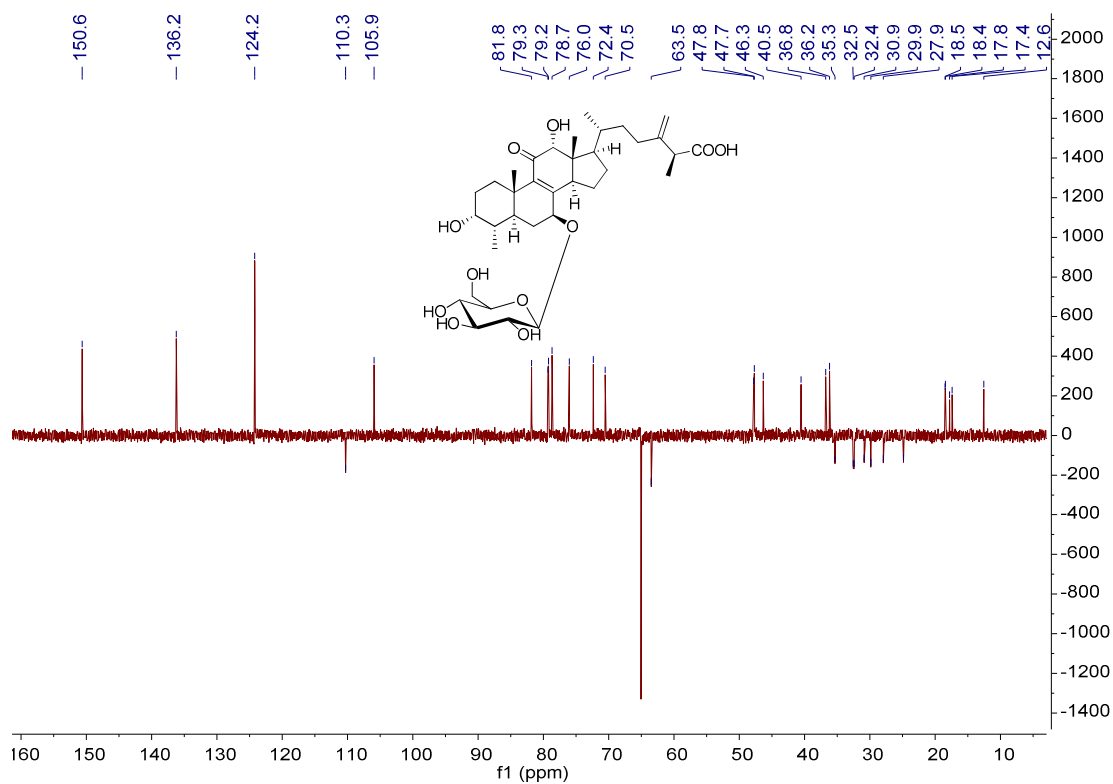


Figure S37. DEPT 135 spectrum of **6a** in pyridine-*d*₅ (100 MHz).

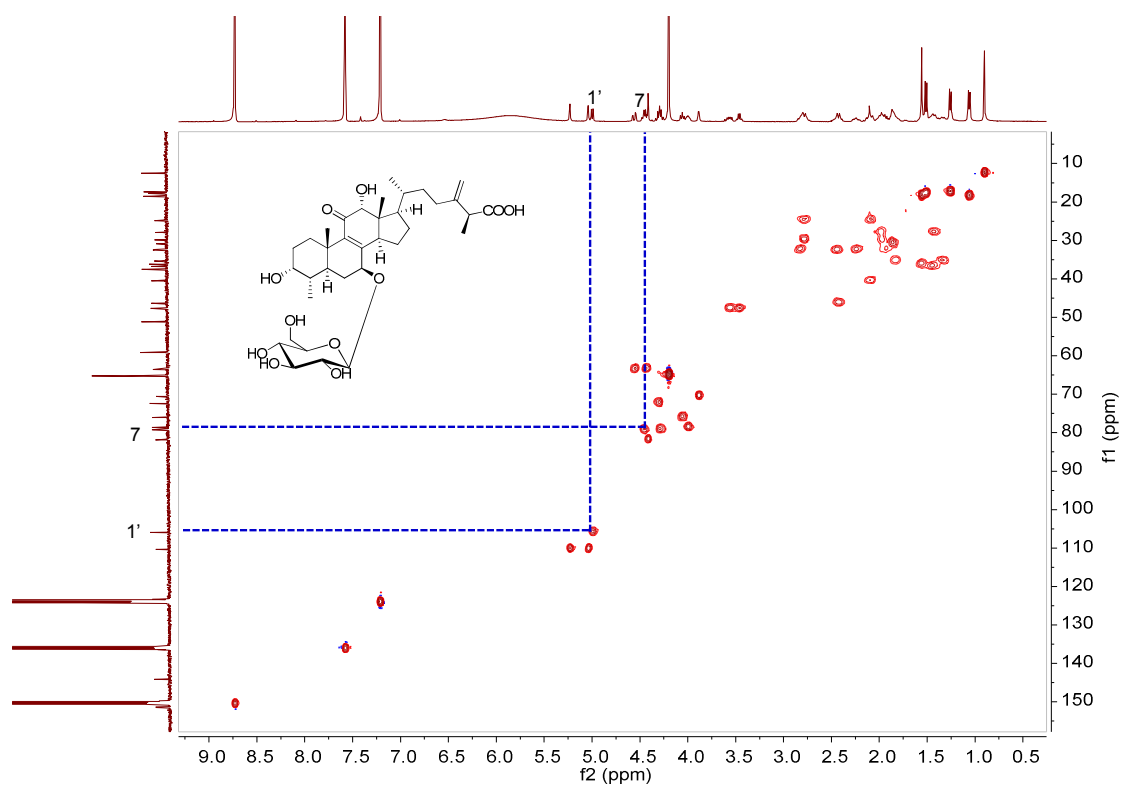


Figure S38. HSQC spectrum of **6a** in pyridine-*d*₅ (400 MHz).

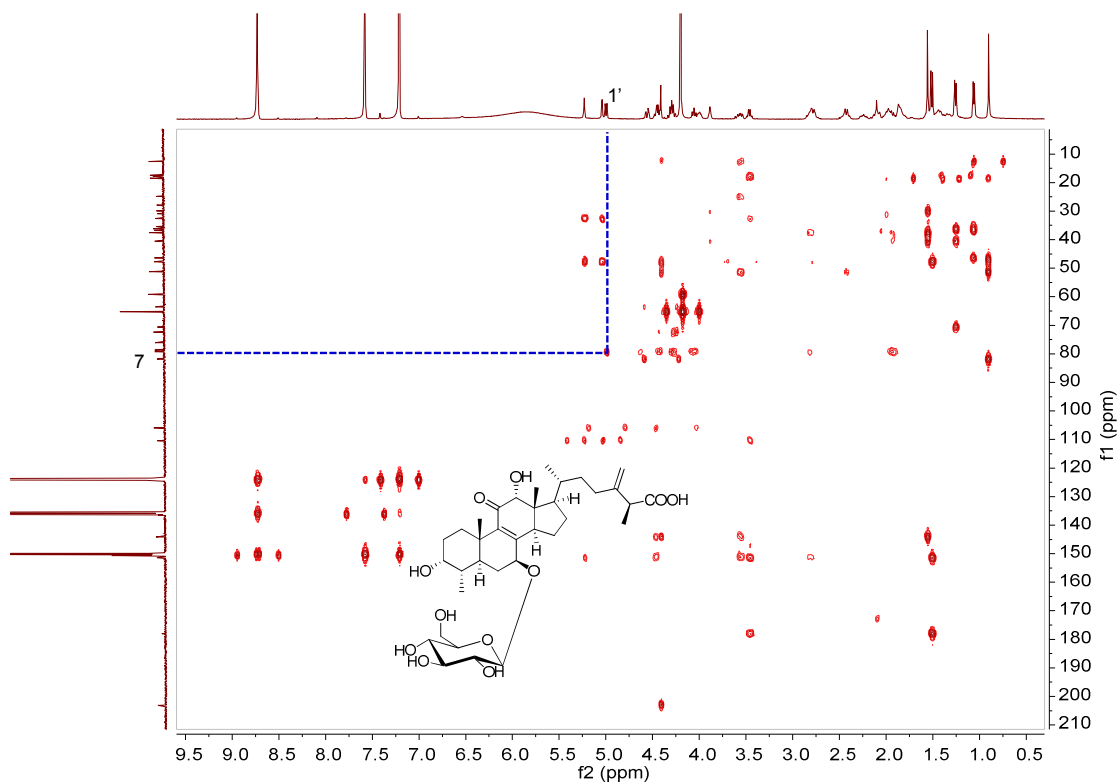


Figure S39. HMBC spectrum of **6a** in pyridine- d_5 (400 MHz).

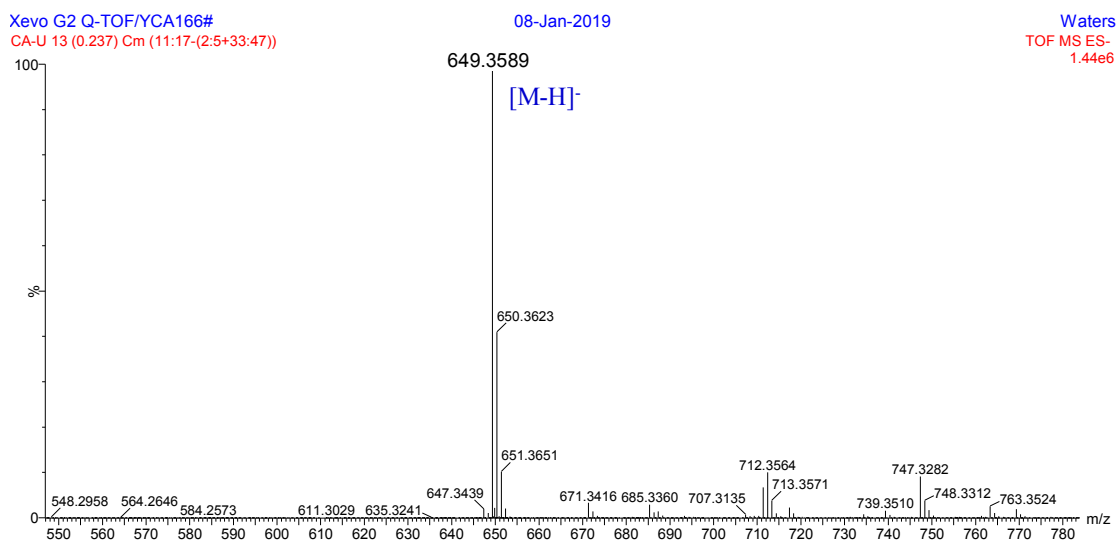


Figure S40. HR-ESI-MS spectrum of **6a**.

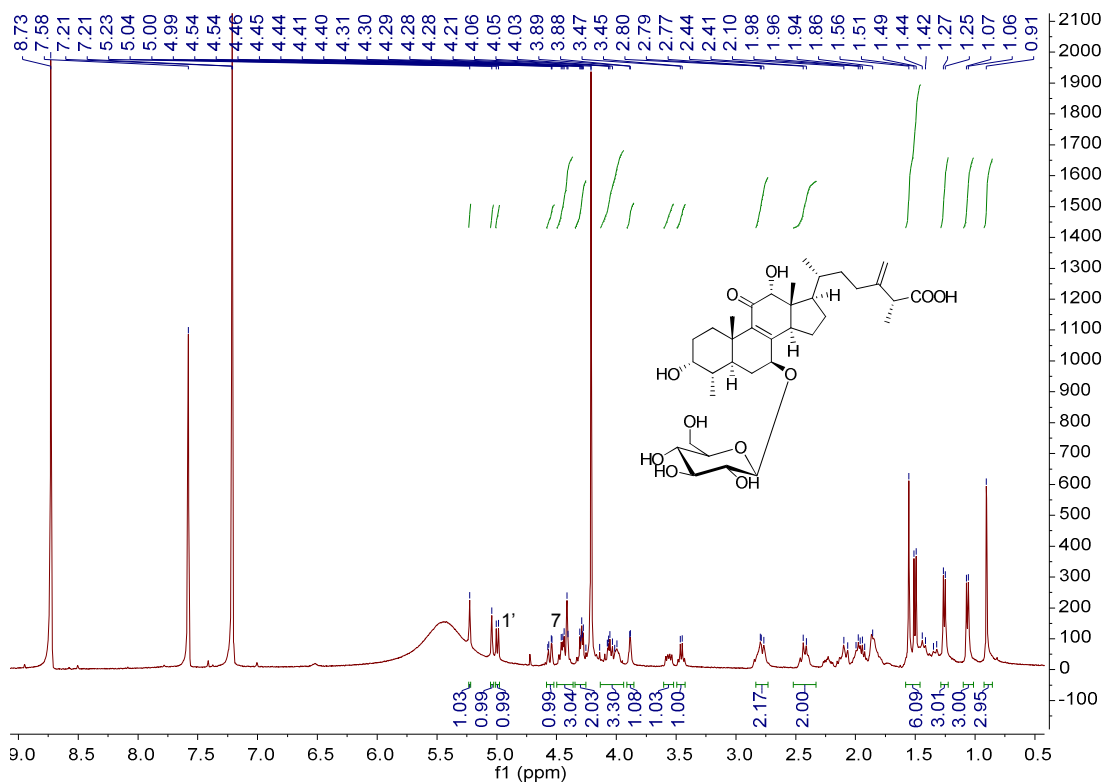


Figure S41. ^1H NMR spectrum of **7a** in pyridine- d_5 (400 MHz).

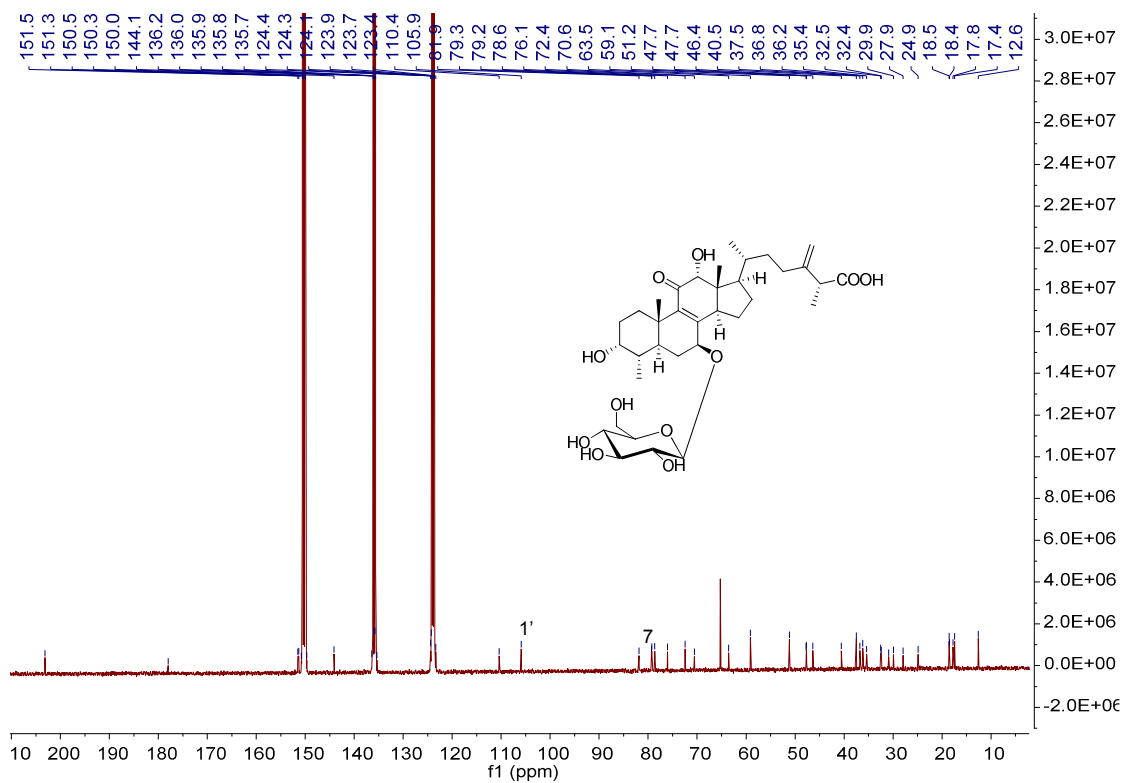


Figure S42. ^{13}C NMR spectrum of **7a** in pyridine- d_5 (100 MHz).

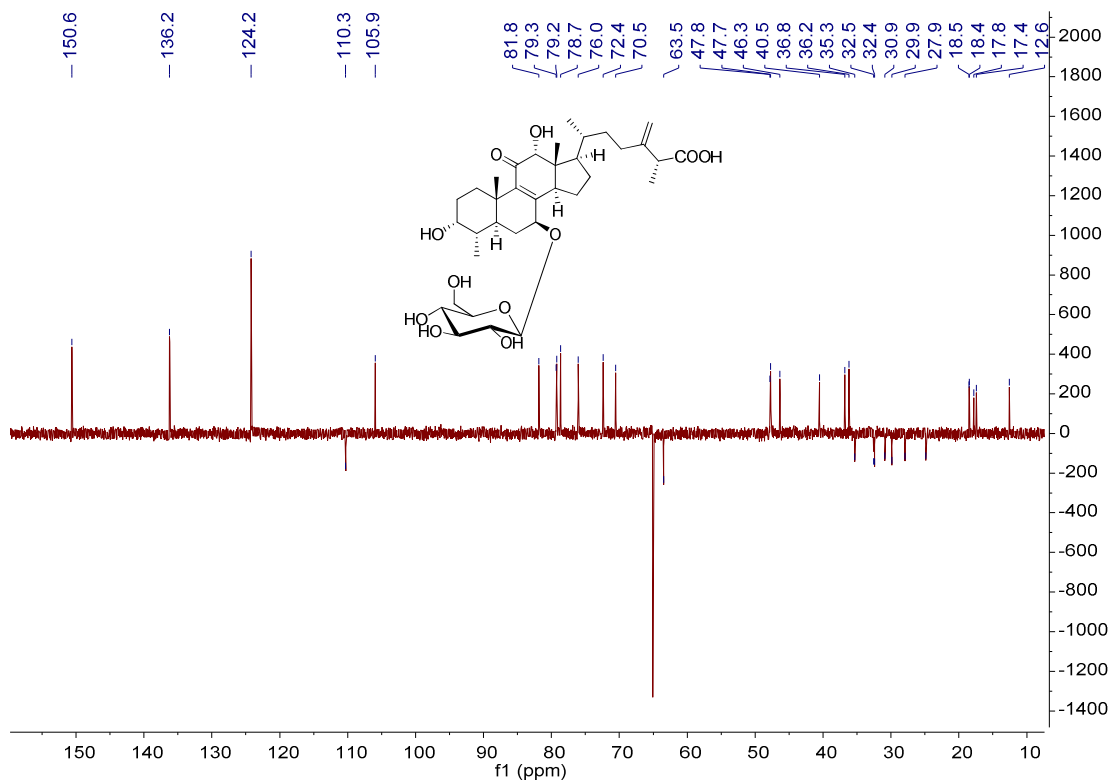


Figure S43. DEPT 135 spectrum of **7a** in pyridine-*d*₅ (100 MHz).

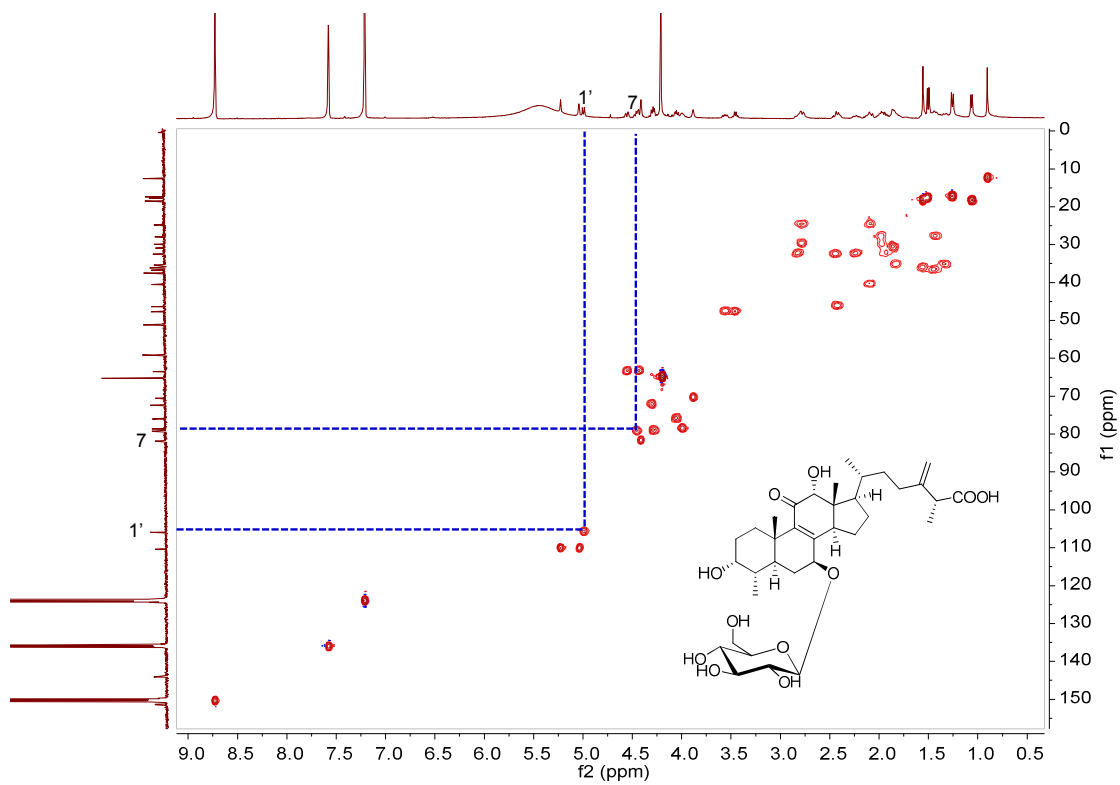


Figure S44. HSQC spectrum of **7a** in pyridine-*d*₅ (400 MHz).

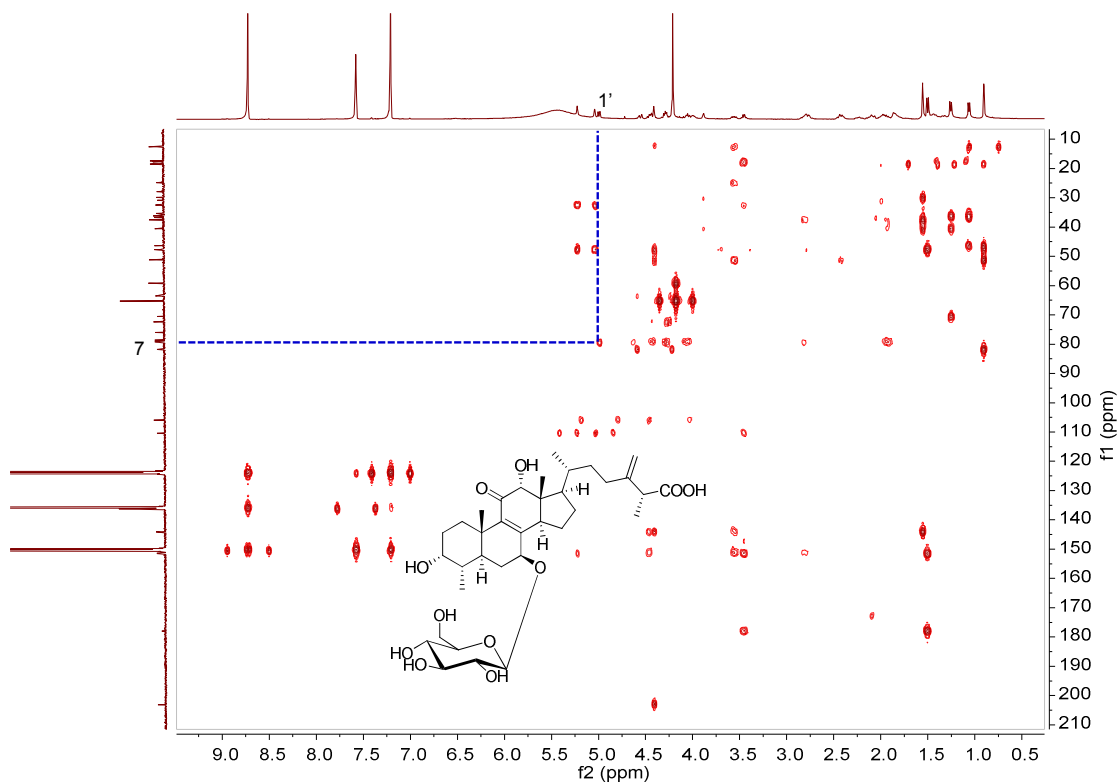


Figure S45. HMBC spectrum of **7a** in pyridine- d_5 (400 MHz).

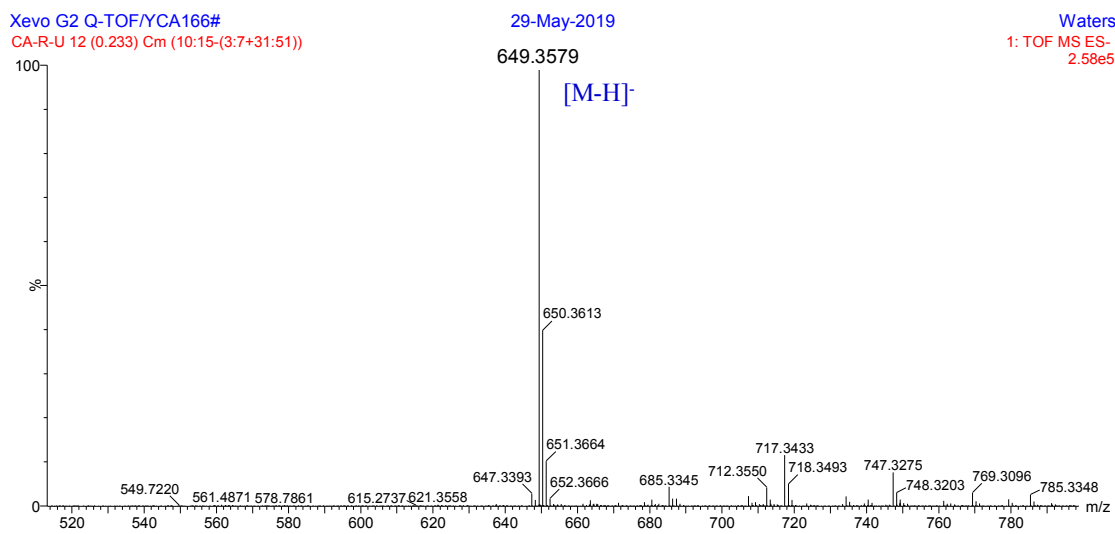


Figure S46. HR-ESI-MS spectrum of **7a**.

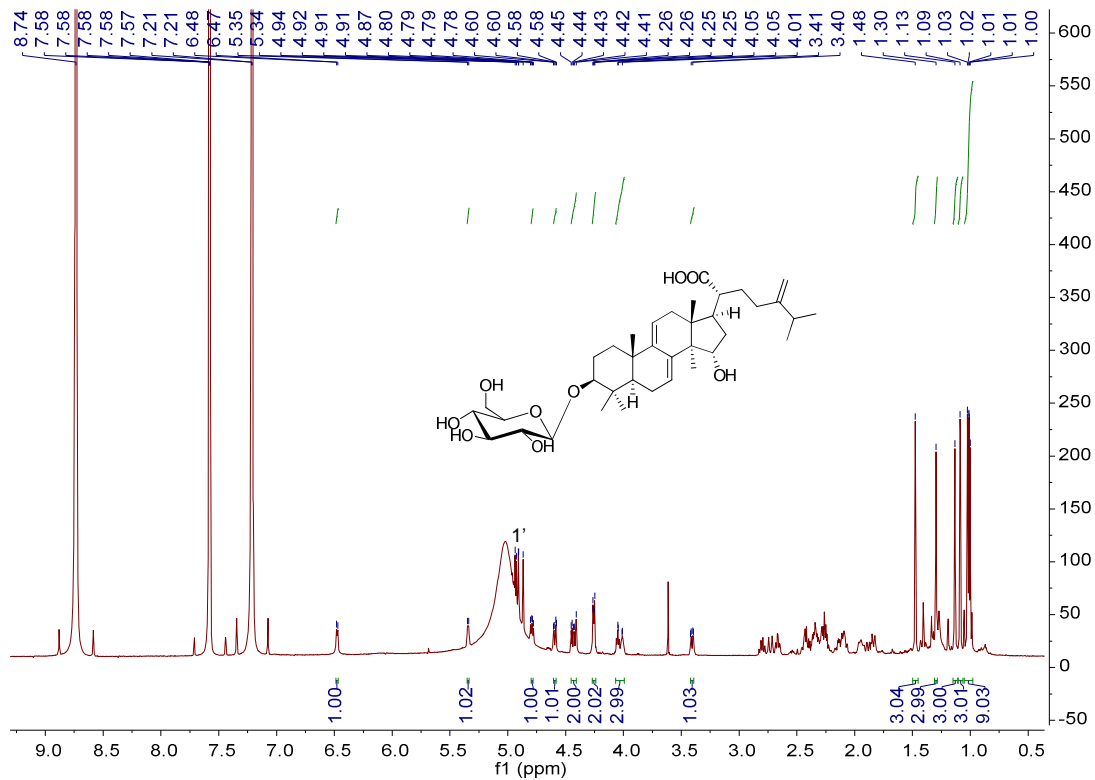


Figure S47. ^1H NMR spectrum of **9a** in pyridine- d_5 (600 MHz).

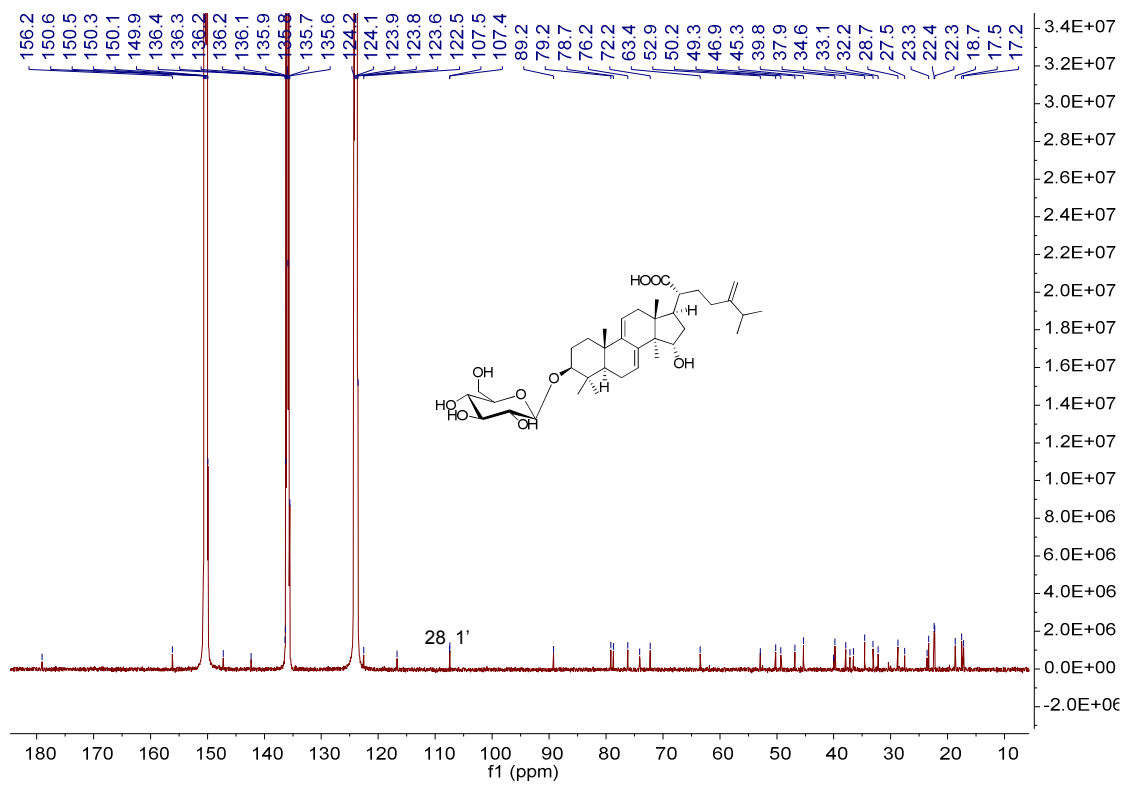


Figure S48. ^{13}C NMR spectrum of **9a** in pyridine- d_5 (150 MHz).

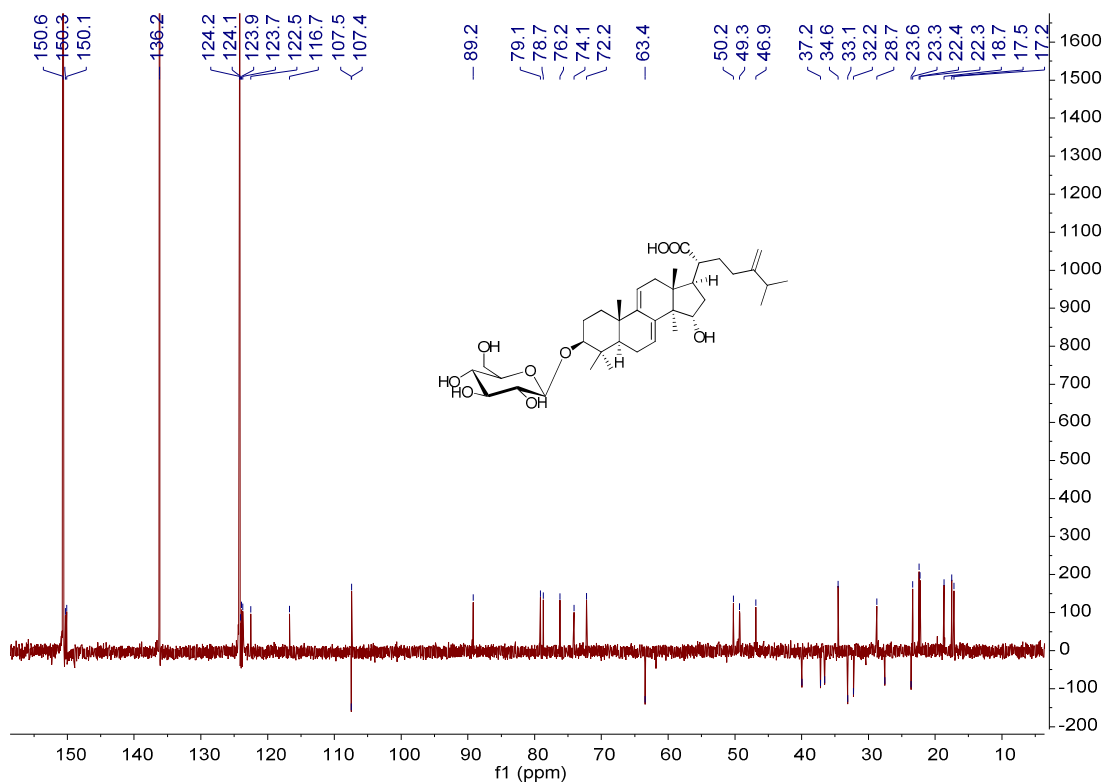


Figure S49. DEPT 135 spectrum of **9a** in pyridine-*d*₅ (150 MHz).

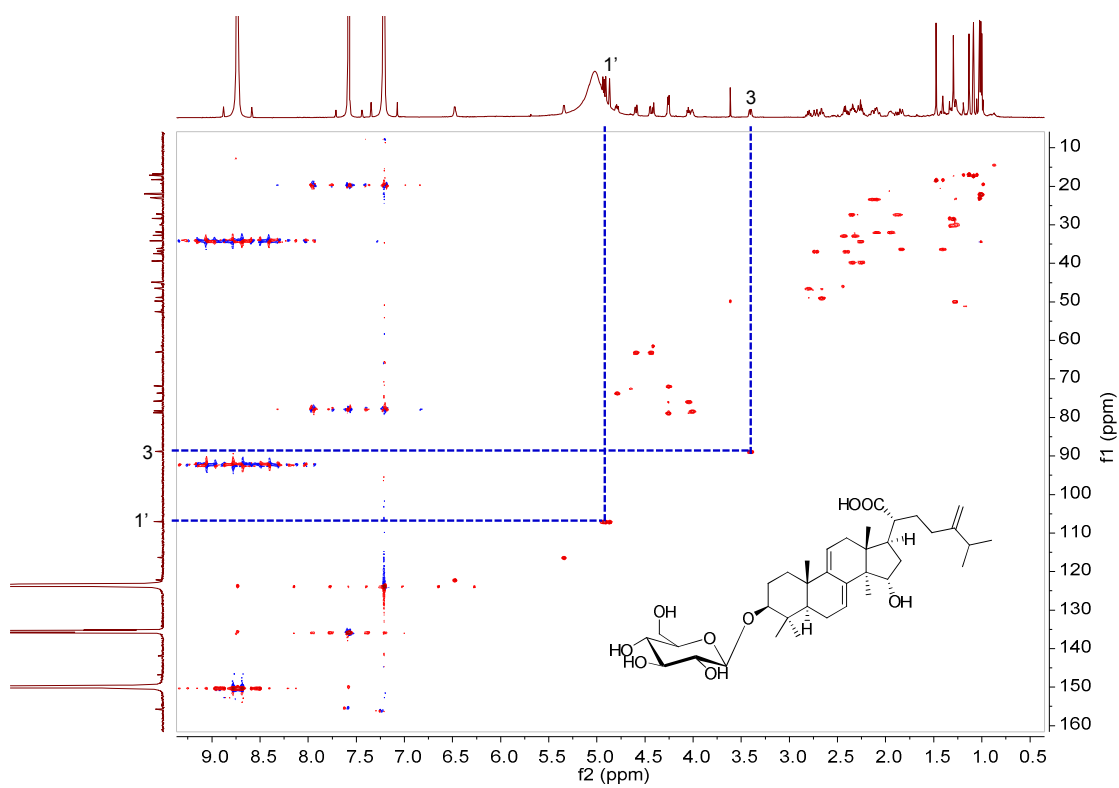


Figure S50. HSQC spectrum of **9a** in pyridine-*d*₅ (600 MHz).

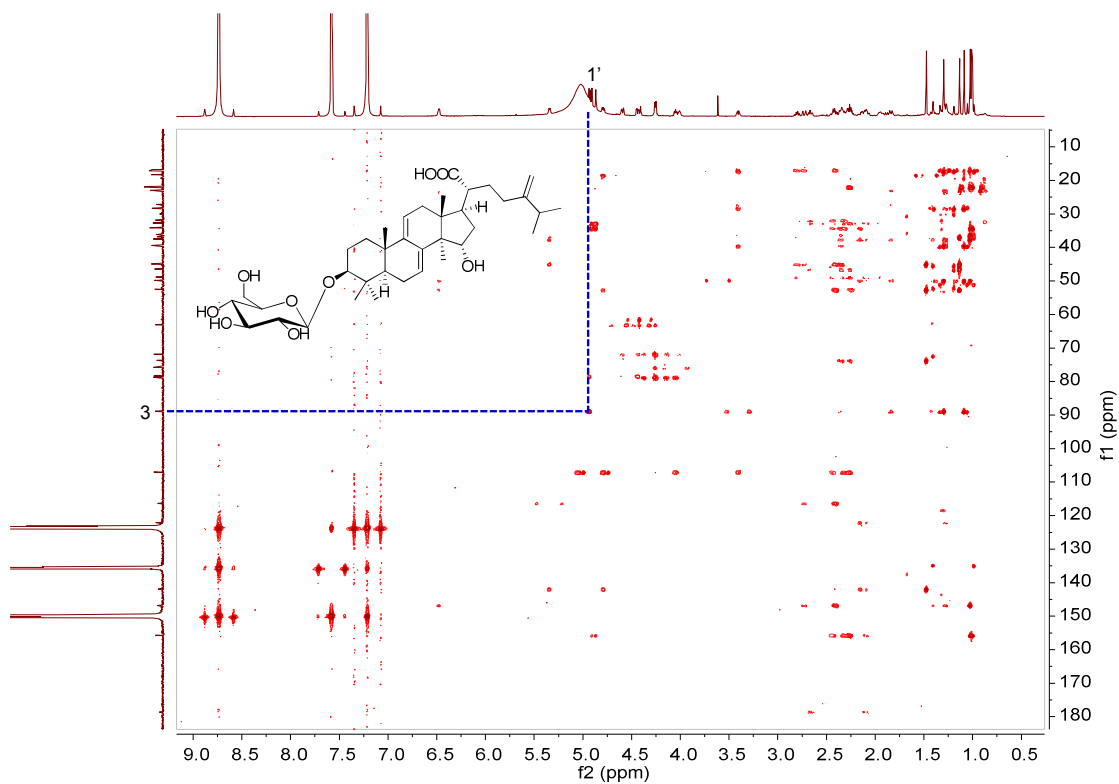


Figure S51. HMBC spectrum of **9a** in pyridine- d_5 (600 MHz).

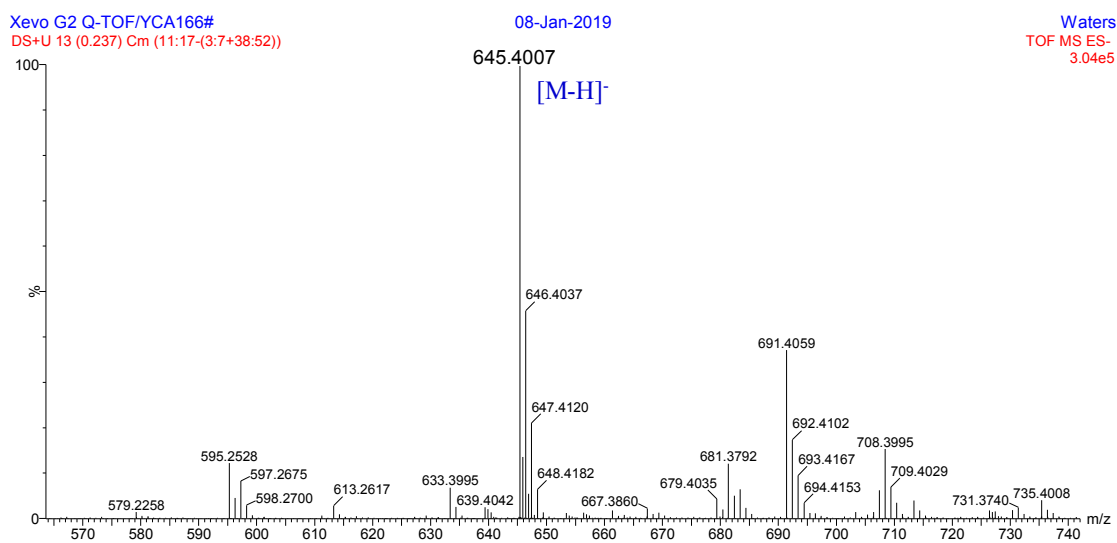


Figure S52. HR-ESI-MS spectrum of **9a**.

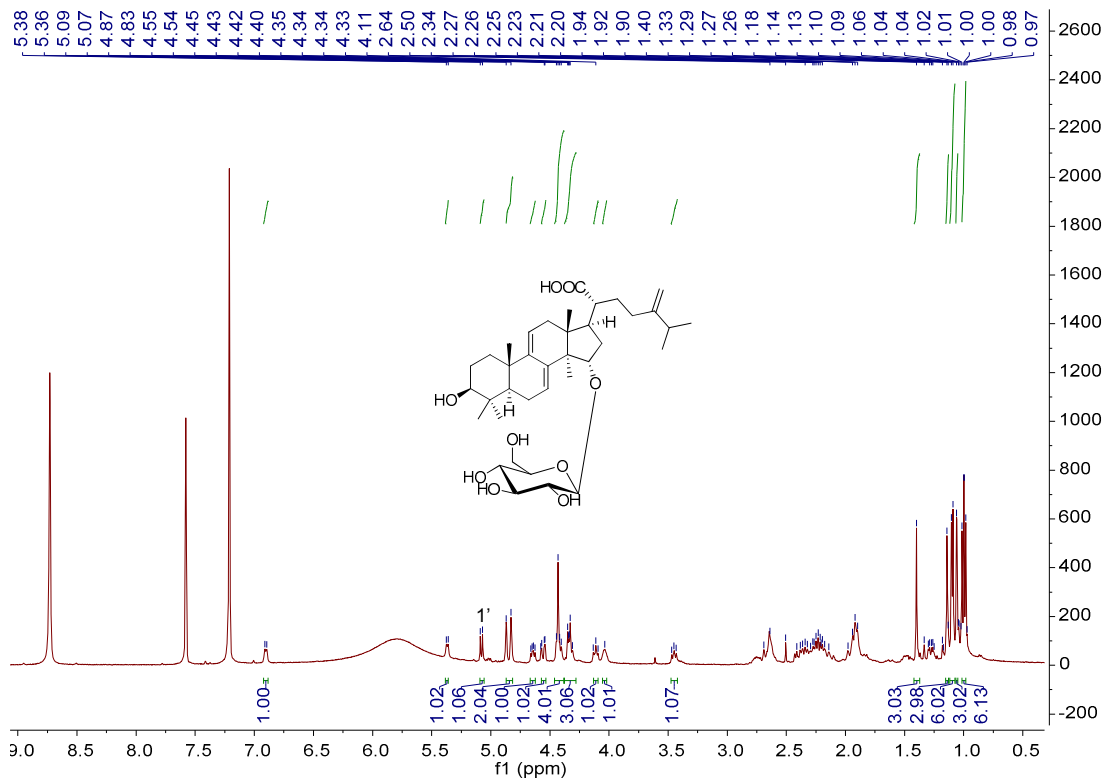


Figure S53. ^1H NMR spectrum of **9b** in pyridine- d_5 (400 MHz).

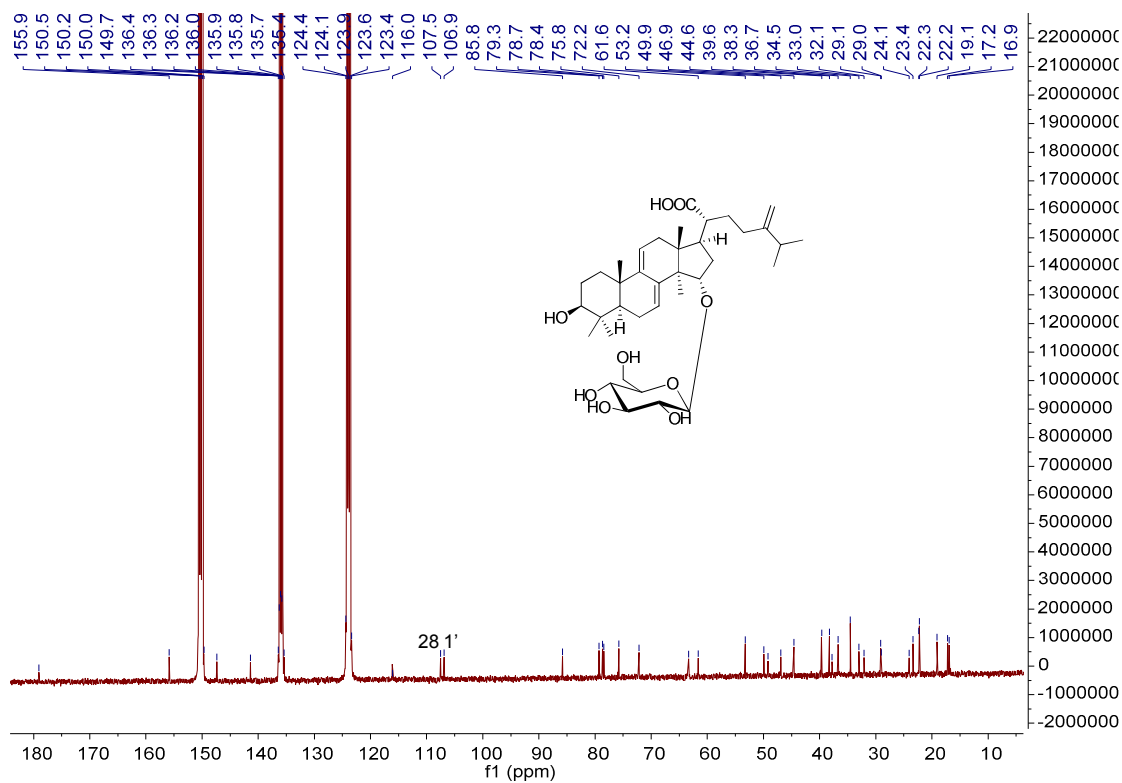


Figure S54. ^{13}C NMR spectrum of **9b** in pyridine- d_5 (100 MHz).

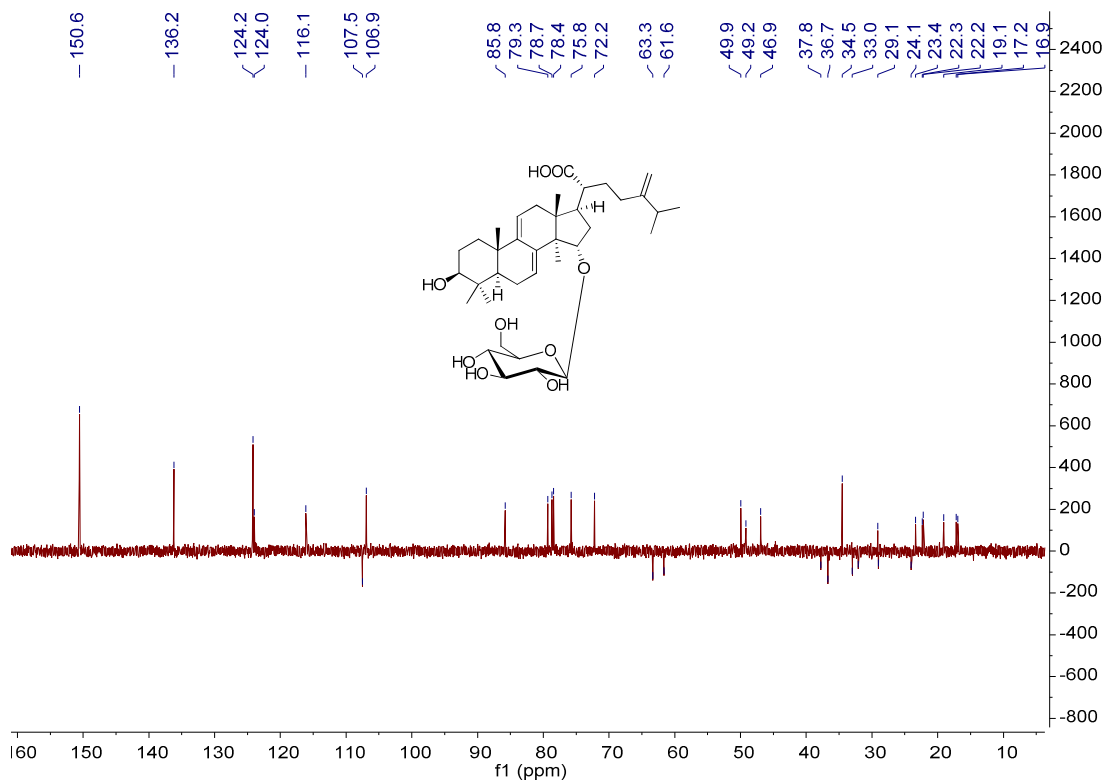


Figure S55. DEPT 135 spectrum of **9b** in pyridine-*d*₅ (100 MHz).

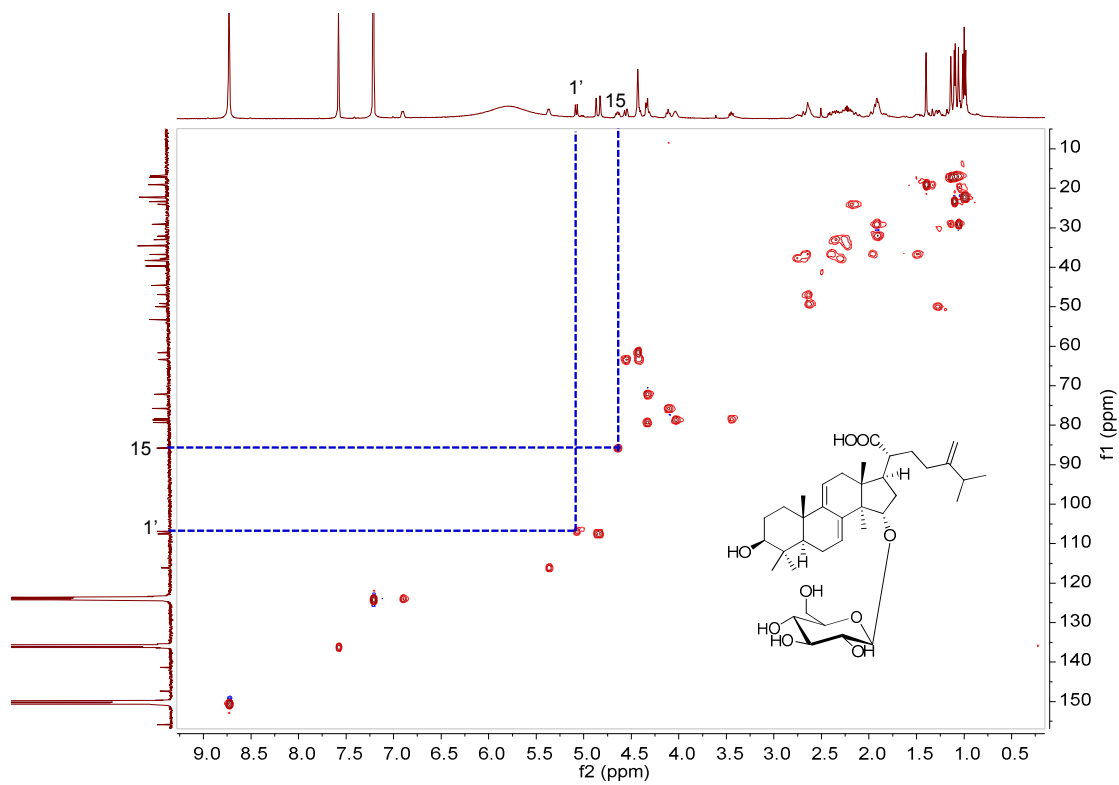


Figure S56. HSQC spectrum of **9b** in pyridine-*d*₅ (400 MHz).

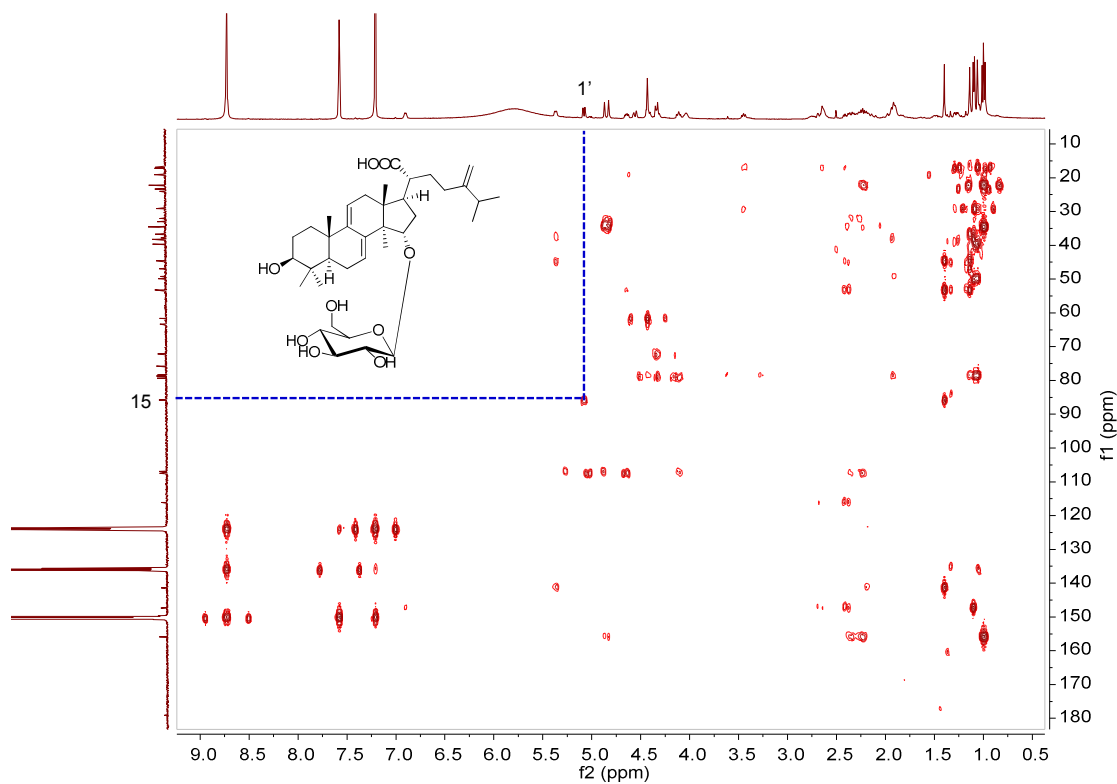


Figure S57. HMBC spectrum of **9b** in pyridine- d_5 (400 MHz).

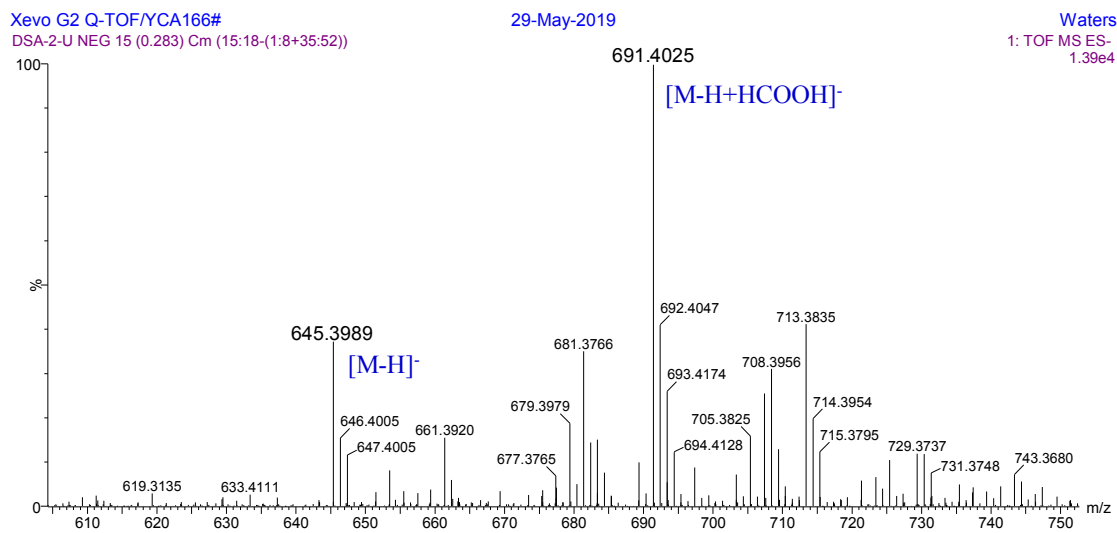


Figure S58. HR-ESI-MS spectrum of **9b**.

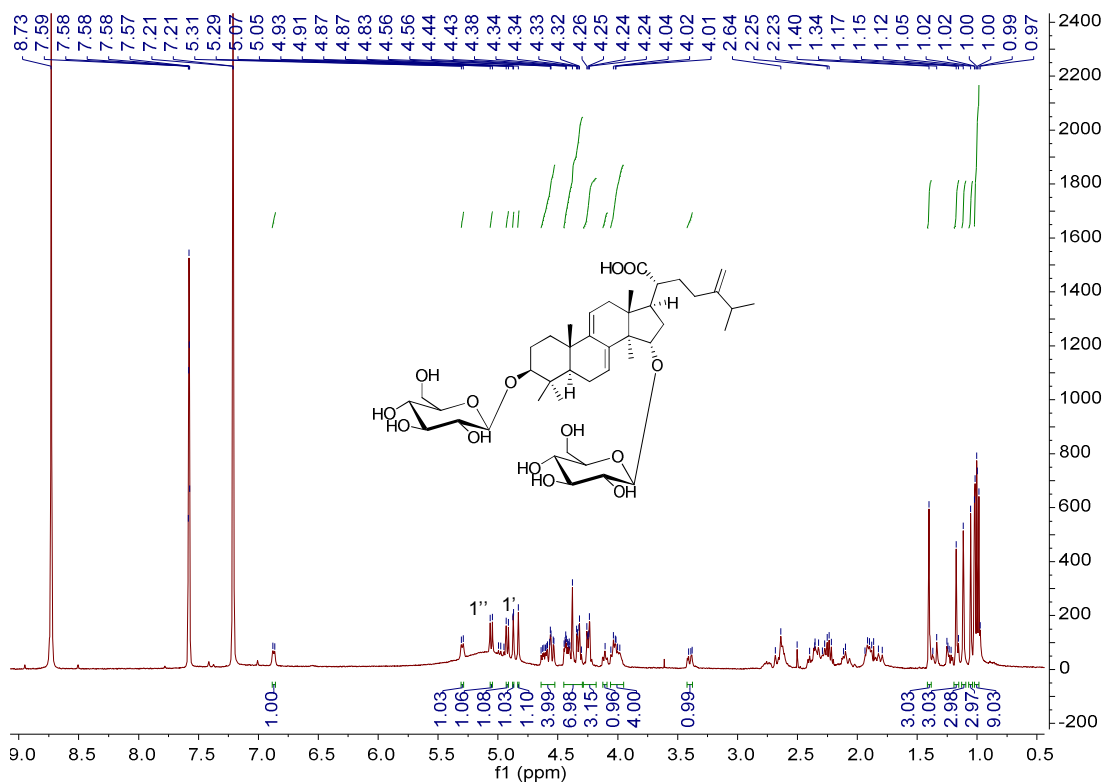


Figure S59. ^1H NMR spectrum of **9c** in pyridine- d_5 (400 MHz).

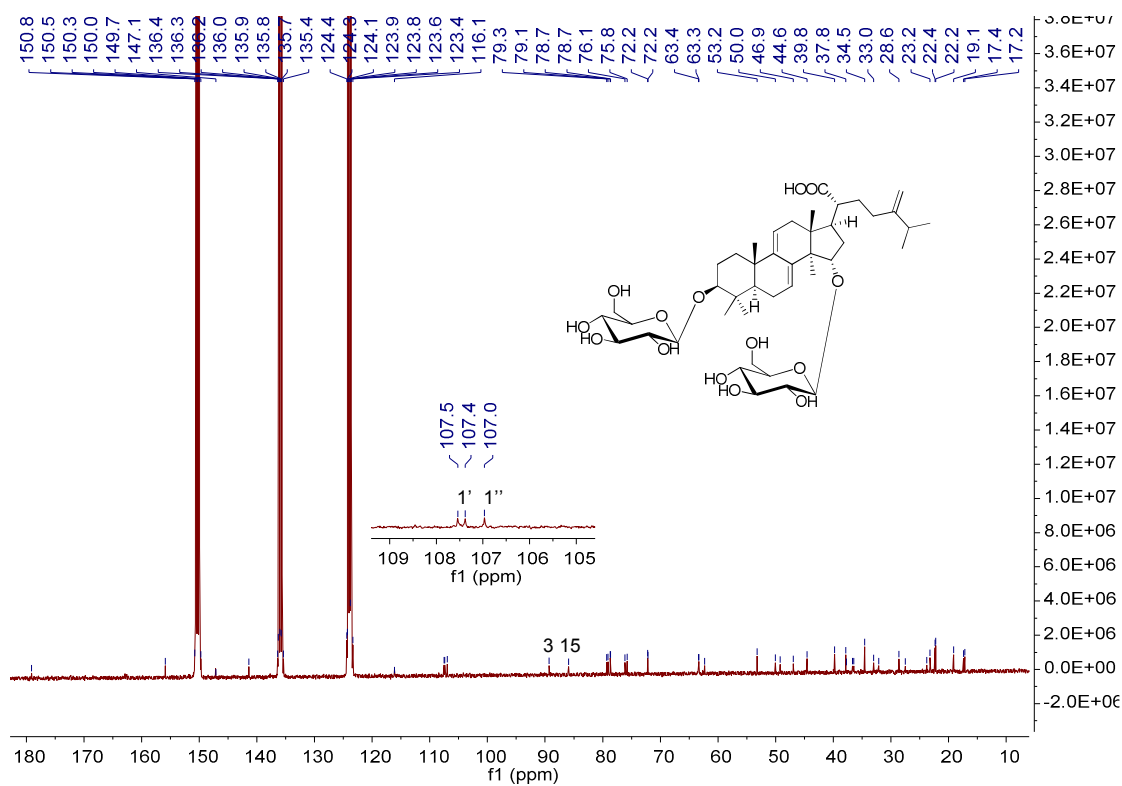


Figure S60. ^{13}C NMR spectrum of **9c** in pyridine- d_5 (100 MHz).

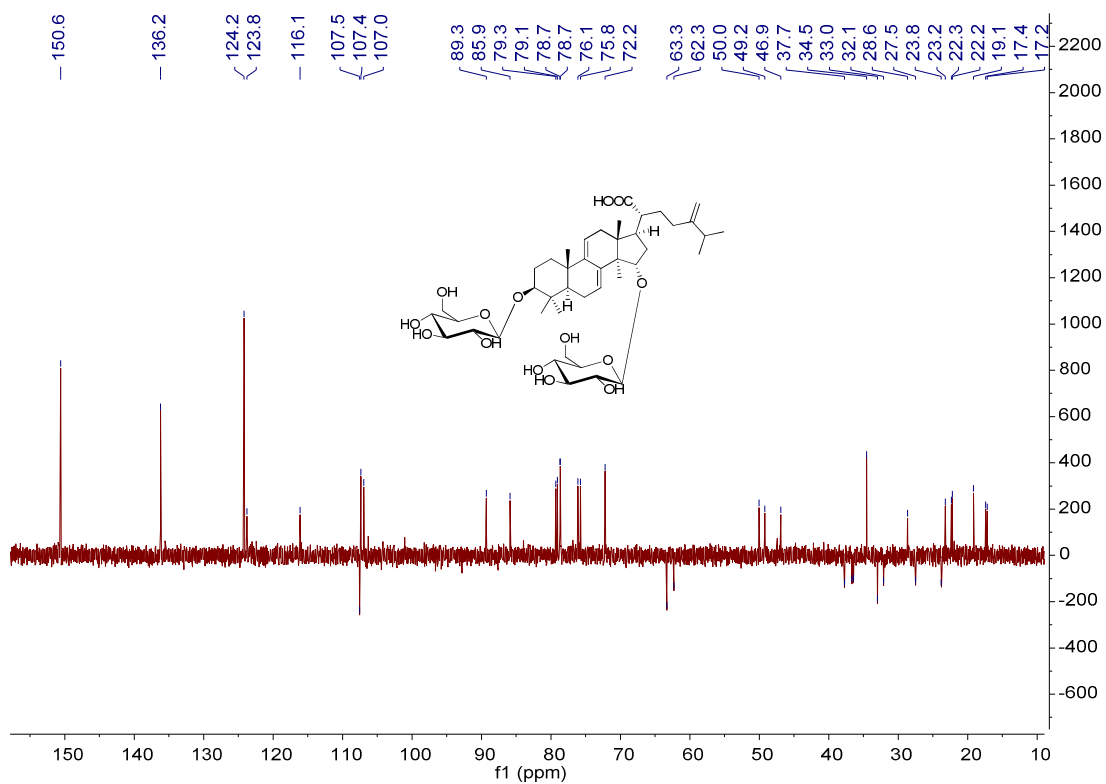


Figure S61. DEPT 135 spectrum of **9c** in pyridine-*d*₅ (100 MHz).

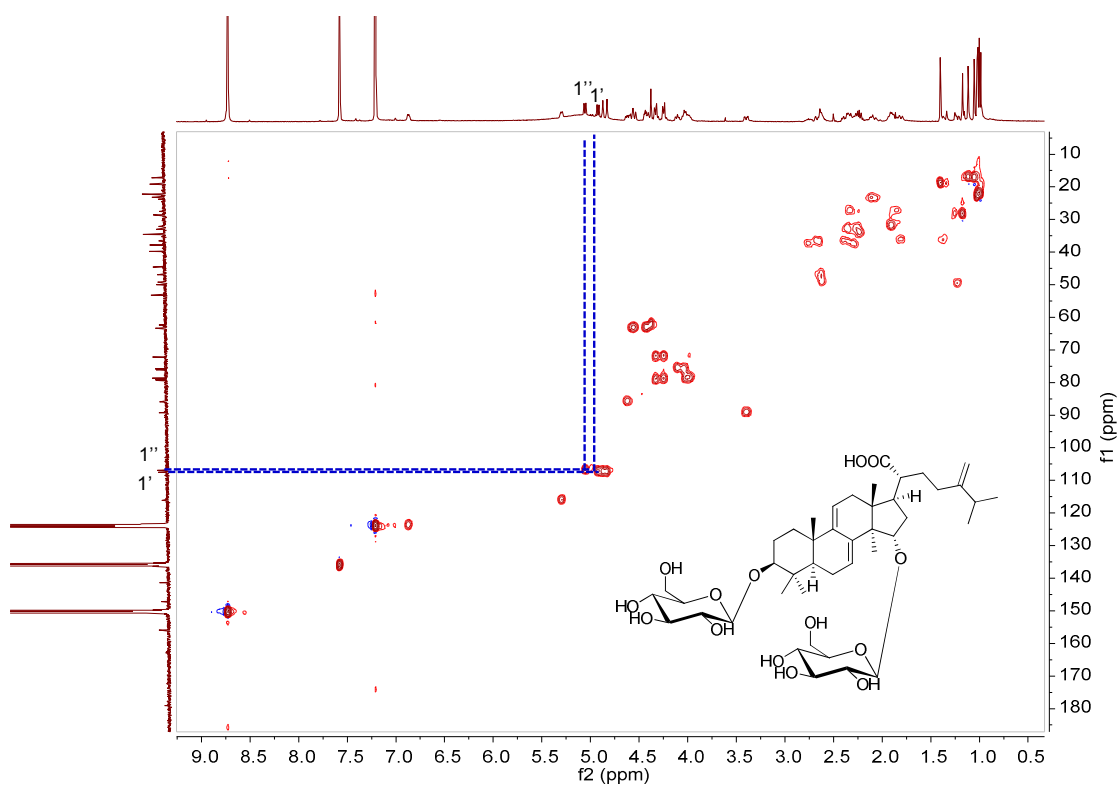


Figure S62. HSQC spectrum of **9c** in pyridine-*d*₅ (400 MHz).

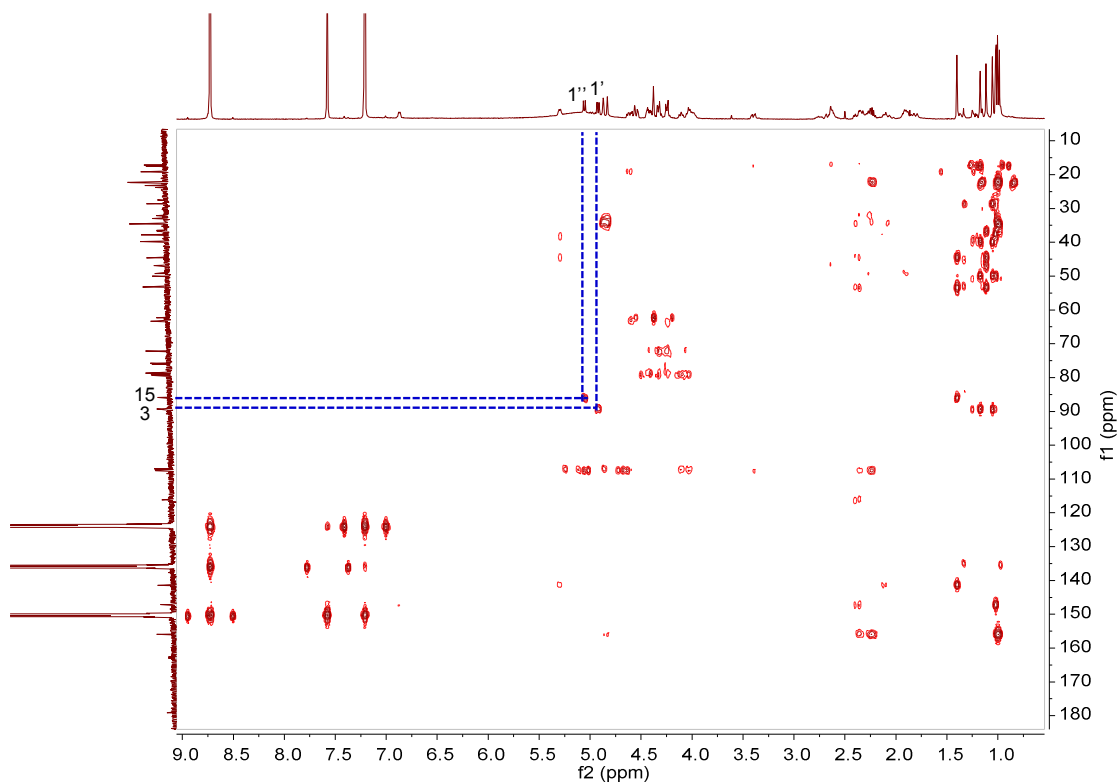


Figure S63. HMBC spectrum of **9c** in pyridine- d_5 (400 MHz).

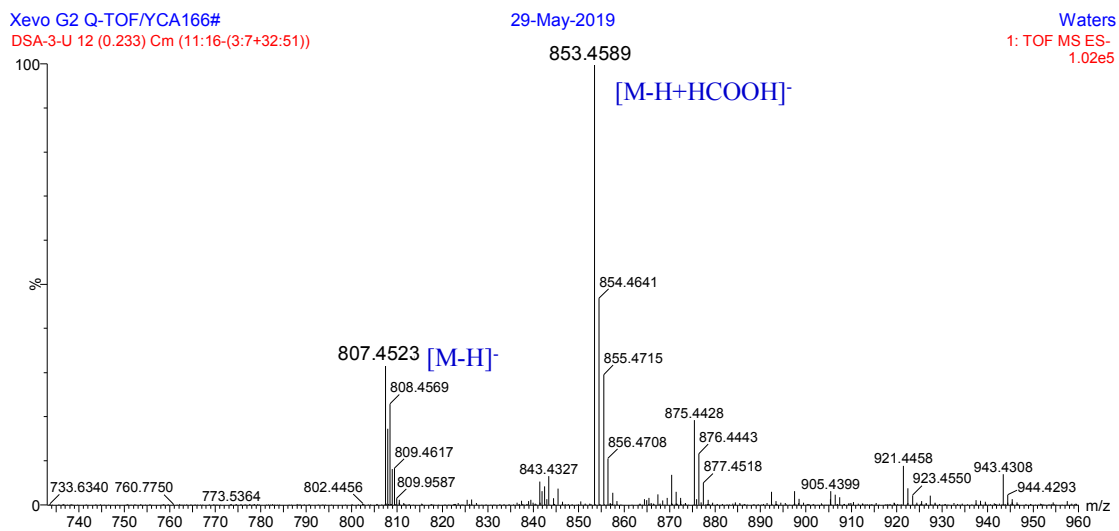


Figure S64. HR-ESI-MS spectrum of **9c**.

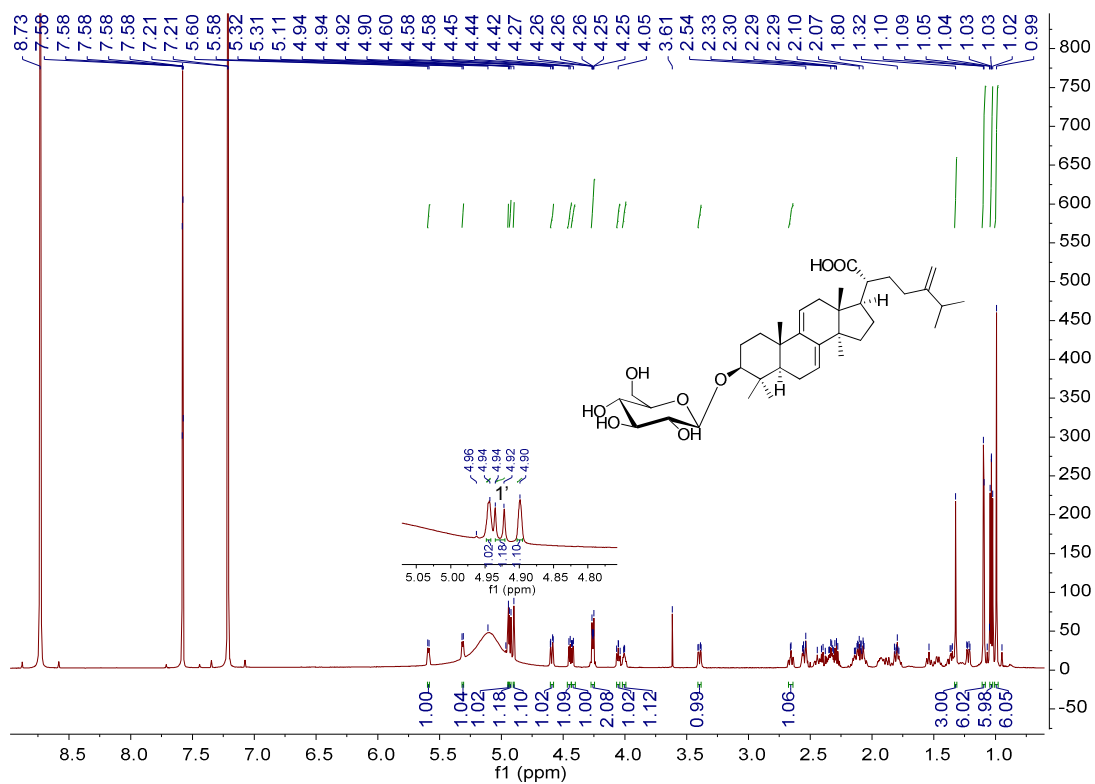


Figure S65. ^1H NMR spectrum of **10a** in pyridine- d_5 (600 MHz).

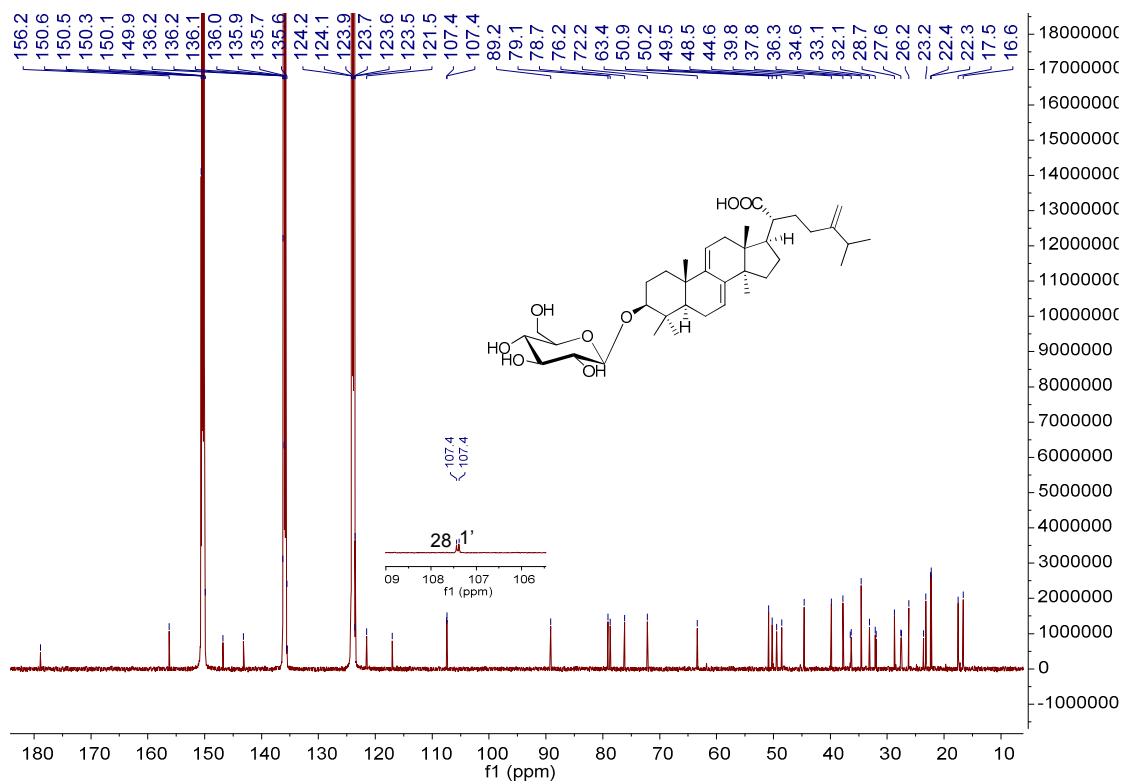


Figure S65. ^{13}C NMR spectrum of **10a** in pyridine- d_5 (150 MHz).

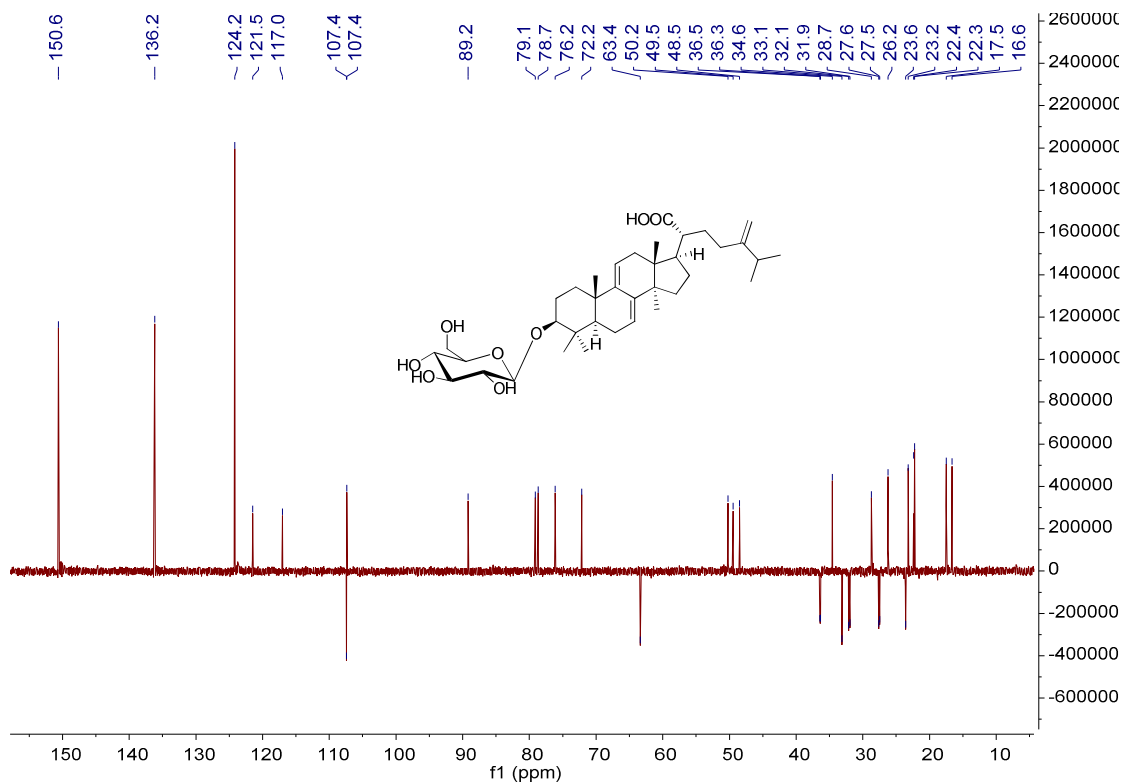


Figure S67. DEPT 135 spectrum of **10a** in pyridine-*d*₅ (150 MHz).

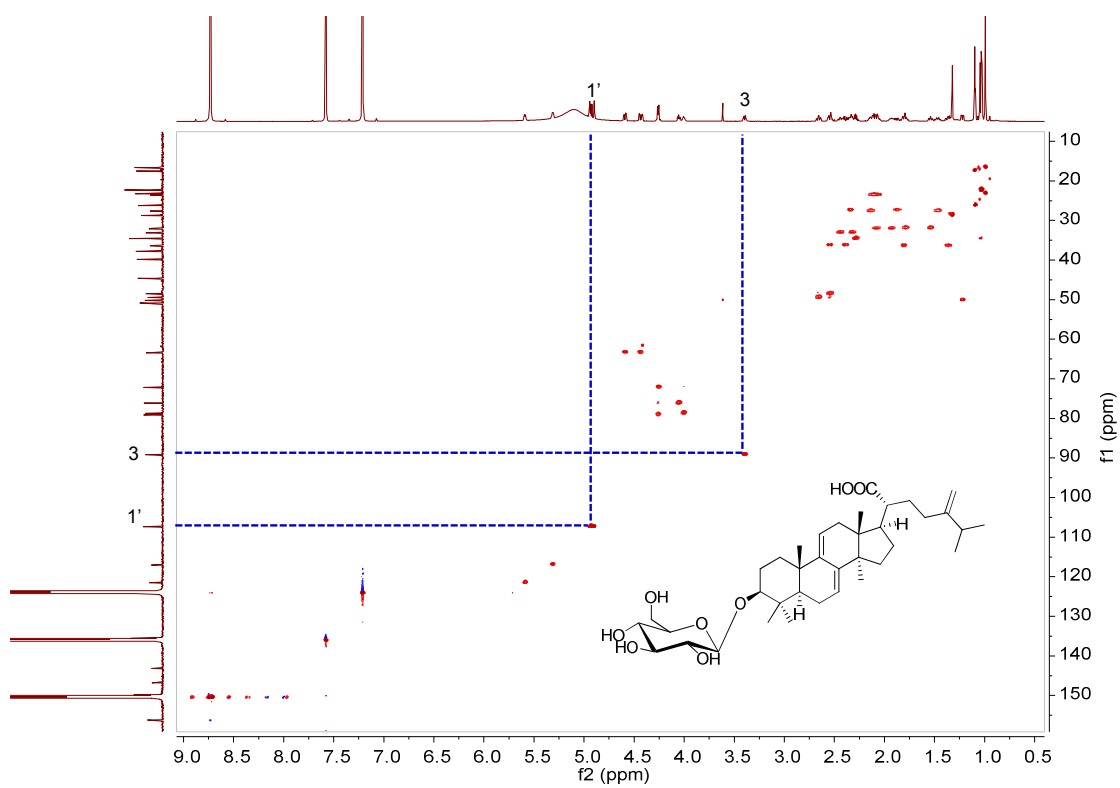


Figure S68. HSQC spectrum of **10a** in pyridine-*d*₅ (600 MHz).

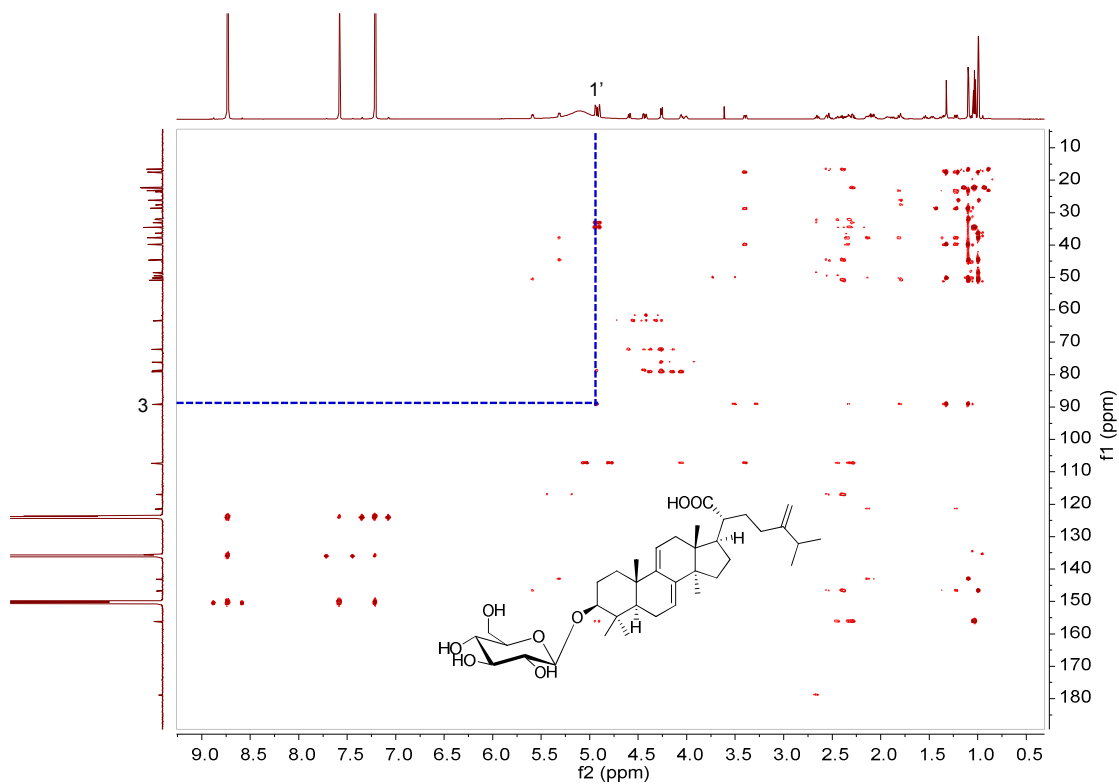


Figure S69. HMBC spectrum of **10a** in pyridine- d_5 (600 MHz).

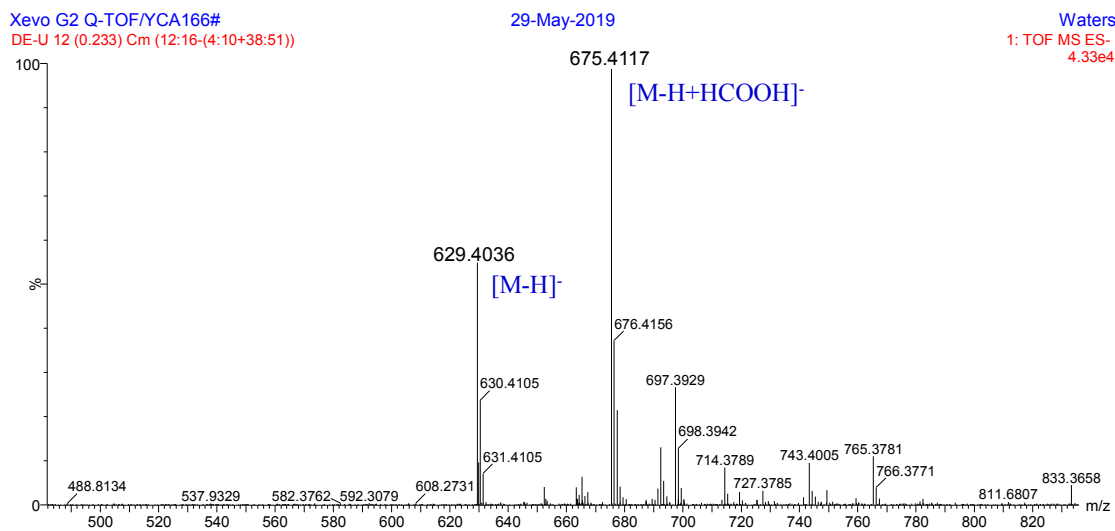


Figure S70. HR-ESI-MS spectrum of **10a**.

References

- [1] B. Li, Y. Kuang, J. B. He, R. Tang, L. L. Xu, C. H. Leung, D. L. Ma, X. Qiao and M. Ye, *J. Nat. Prod.*, 2020, 83, 45-54.
- [2] K. Chen, J. B. He, Z. M. Hu, W. Song, L. Y. Yu, K. Li, X. Qiao and M. Ye, *J. Asian Nat. Prod. Res.*, 2018, 20, 615-623.
- [3] Y. Yi, M. Zhang, H. Xue, R. Yu, Y. O. J Bao, Y. Kuang, Y. Chai, W. Ma, J. Wang, X. M. Shi, W. Z Li, W. Hong, J.-H Li, E. Muturi, H. P Wei, J. Wlodarz, S. Roszak, X. Qiao, H. Yang and M. Ye, *Acta Pharm. Sin. B*, 2022, 12, 4154-4164.